ON THE DRYING MECHANISM OF RADIO-FREQUENCY HEATING

UKICHI SHINOHARA, SHIGEKATSU OTORI AND KOJI IWATA

Department of Electrical Engineering

(Received 30 April, 1952)

1. Introduction.

The object of this paper is to investigate the drying mechanism of radio-frequency heating. Radio-frequency heating is a favorite method for uniform heating of bad conductors of heat, because heat is generated by dielectric loss in each molecule of the substance tested. The dielectric loss per unit volume is

$$P=2\pi f C_0 E^2 \cdot \varepsilon \cdot \tan\delta \times 10^{-12} \quad \text{watts/cm}^3, \tag{1}$$

where, f : frequency of the applied electrical field in cycles per second,
E : electrical field intensity in volt per centimeter,
C_0: capacity per unit volume in vacuum in farads,
ε : dielectric constant,
$\tan\delta$: dielectric power factor.

In applying this phenomenon to any material for industrial use, there are many unknown subjects requiring further inquiry. For instance, the dielectric characteristics of the material for industrial use; the relation between its size and the frequency of applied field; the arrangement of electrodes; the construction, the stability, and the load matching of the high frequency oscillator; the interference with the radio broad-cast; etc. must be studied. The subjects concerning the electrical phenomena are discussed in "The Theory and Application of Radio-Frequency Heating" by C. H. Brown, C. N. Hoyler and R. A. Bierwirth (1948), "The Latest Radio-Frequency Applications I (1949), and II (1951)" compiled by Yamamoto; and "Radio-Frequency Heating" compiled by Saito, etc.. In this paper we shall explain the drying mechanism of radio-frequency heating and fundamental ideas in designing drying apparatuses for radio-frequency heating. And a supplementary explanation will be added of the dielectric characteristics of various materials for industrial use, together with some data amassed from the practical applications of radio-frequency heating to industrial works.

2. On the Drying Characteristics of Clay.

Concerning the drying characteristics of clay, the researches[1] by Prof. Kamei and Prof. Kato of Kyoto University are confined only to the range of wave length from 1.2 m. to 2 m., in which experiments they used a magnetron oscillator (1 kw.), but in our laboratory we studied not only into the drying characteristics at different frequencies (1~200 MC), but also into those at different high frequency powers. From the results obtained in those experiments, we are going to draw

conclusions about the allowable electric power density for drying test pieces, and the fundamental ideas in designing high-frequency osciliators and drying apparatuses. We first took up clay as a test piece, and experiments were performed in a box with asbestos walls as shown in Fig. 1. This box enabled us to control the surrounding temperature and humidity so that they might be in the desired condition. The test piece used was the clay of the moisture content of about 27%, which is used for the manufacture of electrical insulators at the Nippon Gaishi Co. Ltd., and this was cut out into a cylinder, 6.8 cm. in diameter and 3.0 cm. long. The oscillators of two tubes RT-356 connected in push-pull, (output: about 5 kw, and frequency range: 5~50 MC) and those of two tubes T-311 connected in push-pull (output: about 300 W., and frequency range: 75~200 MC) were used. The amount of water evaporated from the test piece was continuously measured by weighing the test piece in the balance. The percentage of moisture content at any time has been calculated from the following relation:

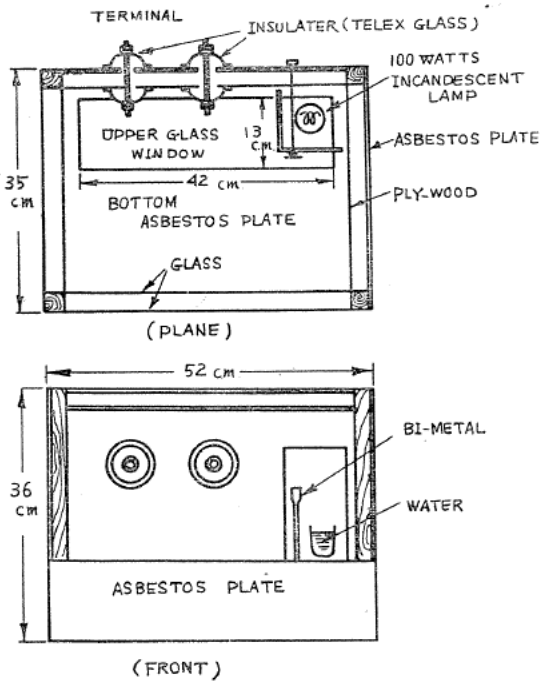

FIG. 1

$$\frac{W-W_0}{W_0}\times 100\%, \qquad (2)$$

where W_0 is the weight of the substance dried for a long time until it comes to constant weight, and W the weight at any time. The drying rate is indicated by the weight of water evaporated from the surface of the test piece per unit area per unit time, but the correction due to the shrinkage of the test piece is made from the shrinkage curve (Fig. 2), by the following relation:

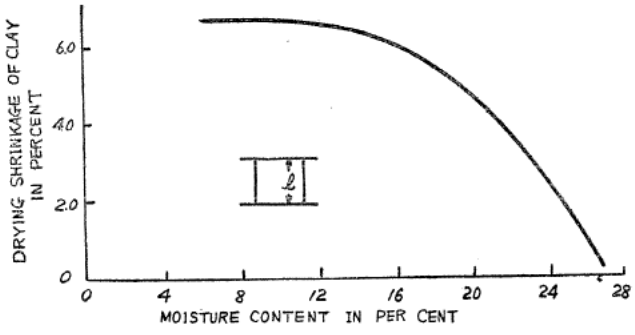

FIG. 2

$$\frac{l-l'}{l}\times 100\%, \tag{3}$$

where, l is the initial length of the test piece, and l' is the length of it at any time. When the test piece of clay was heated by the radio-frequency field of the plane parallel electrodes, (dia. of the electrode being 10.5 cm., frequency 6.7 MC), the results as shown in Fig. 3 were obtained. In this experiment, the considerable variations of high frequency voltage (V), and current (I) were observed during the

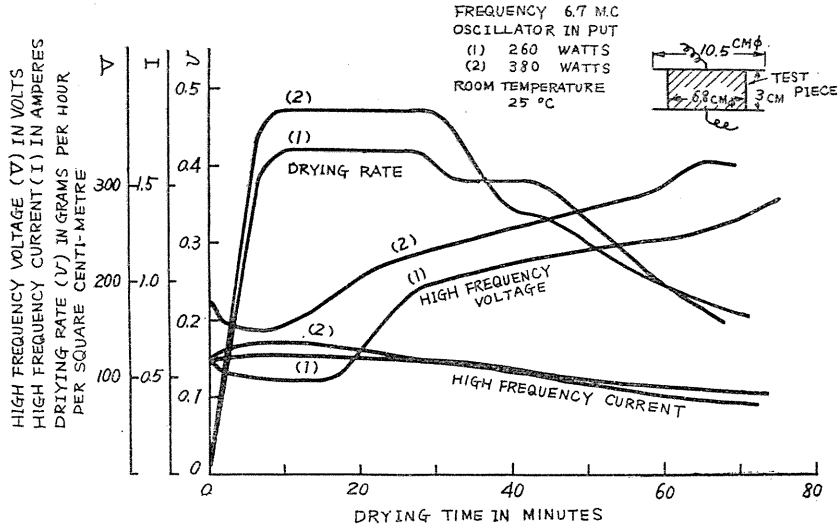

FIG. 3

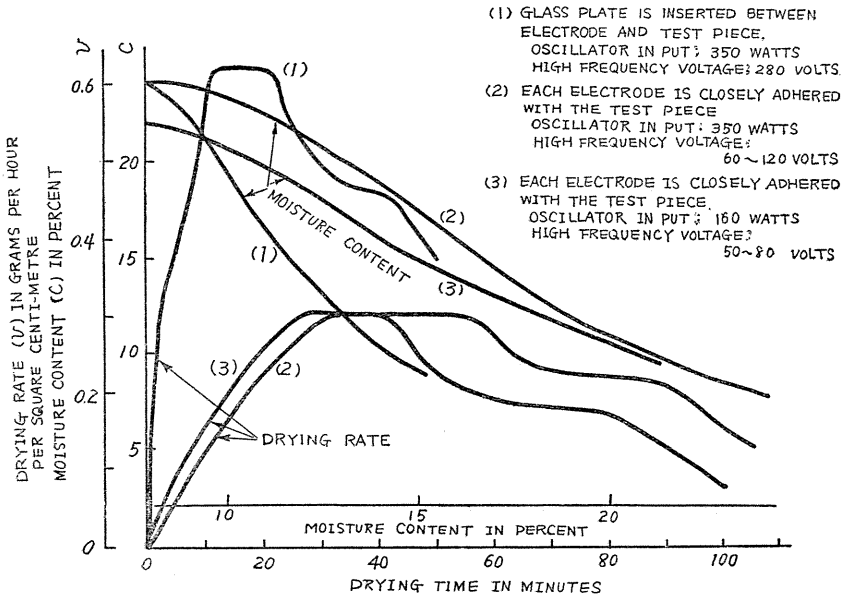

FIG. 4

drying period. We inserted a piece of glass plate, 1.5 mm. in thickness, between the electrodes and the test piece. To ascertain the effect of the said glass plate, we compared the drying characteristics in the above case with those observed when the electrodes were placed in close contact with the test piece, and thus the results shown in Fig. 4 have been obtained. It has been found that the tendency of drying characteristics does not so much differ between these two cases except in the numerical value of the drying rate. The curve obtained when we place the electrode in close contact with the test piece, (the curve (1) in Fig. 4) rises more sharply than when a glass plate is inserted (curve (2) in Fig. 4). Perhaps, this is due to the higher potential gradient and Joule's loss due to conduction current. When the experiment was made at the same drying rate, the relations as indicated by the curves (2) and (3) in Fig. 4 could be obtained. That is, we scarecely find any difference in the tendency between them. Therefore, we examined chiefly the case of the glass plate inserted between the electrodes and the test piece. When electric power was small, a few differences were discovered between the drying characteristics of radio-frequency heating and those of oven-heating, as shown in the curve (1) in Fig. 5. In other words, the pre-heating-period (AB),

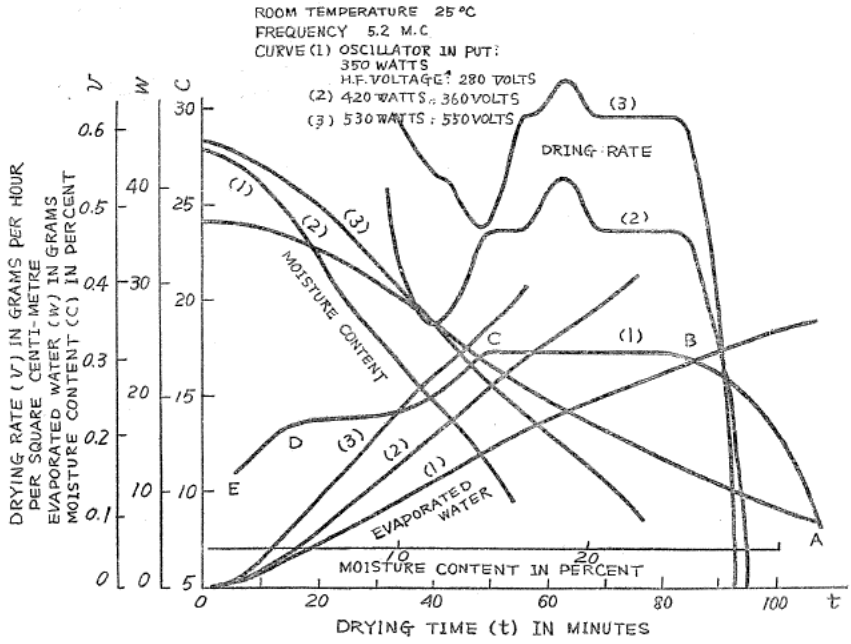

FIG. 5

the constant drying rate period (BC), the first stage of the decreasing drying rate period (CD) and the second stage of the decreasing drying period (DE) follow one after another in this order. But, when radio-frequency heating was used, the drying rate became greater and the decreasing rate period shorter than in the case of oven-heating. When electric power was increased, however, the drying rate was found to become greater, and at last to jump up at the period of decreasing drying rate, and an "internal explosion" took place. When the electric

power was further increased, the phenomenon of the "internal explosion" could be brought about even at the period of the constant drying rate or that of the pre-heating drying rate. Fig. 6 shows the drying characteristics in the case of the "internal explosion" that takes place at the period of the pre-heating drying rate, and the internal surface of the test piece has in this case many radial traces as shown in Fig. 7.

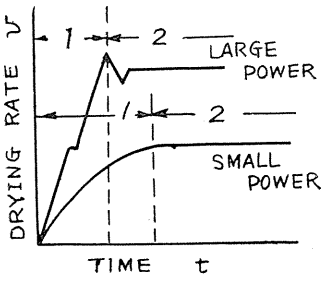

FIG. 6

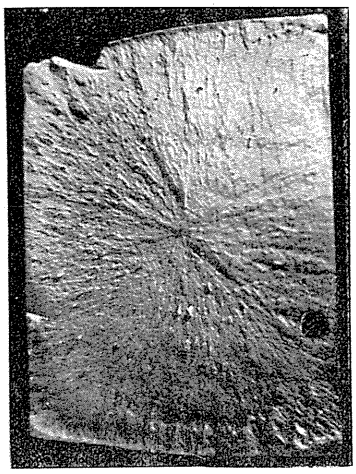

FIG. 7

It is necessary to dry the substance in great speed, but without any defects caused in it. Therefore, the "internal explosion" and "surface cracks" must be avoided. Hence, the amount of the electric power to be transferred into the drying substance and the surrounding temperature and humidity about it must be kept within proper limits.

3. Some Electrical Factors affecting the Drying Characteristics of Radio-Frequency Heating.

(1) *The Effects due to the Electrical Conductivity of the Test Piece.*

In order to investigate the effects due to the different electrical conductivity of the test pieces, the solutions of NaCl of various concentrations (0 Normal, 0.4 Normal and 0.86 Normal) were mixed with clay. The results obtained with these test pieces are shown in Fig. 8. It has been found that the electric current becomes larger with the increased conductivity of the test piece, while the drying rate becomes considerably smaller, that is, the clay of moisture content of 30% is heated rather by dielectric loss than by Joule's loss due to the conduction current.

(2) *The Effect of the Clearance between the Plate Electrodes and the Test Piece.*

When the plate electrodes were separated from the bottom surfaces of the test piece to the distance of δ centimeter, the surface of the test piece from which water evaporated was found to grow larger than when the electrodes were placed in close contact with the test piece, but the electric power transferred into the test piece become smaller. Dr. E. S. Winland[2] says that the transfer efficiency

becomes smaller as the clearance (δ) is made wider. The relation between the drying characteristics and the clearance was experimented and the results as shown in Fig. 9 were obtained. The drying rate decreased as the clearance increased and the drying period became longer.

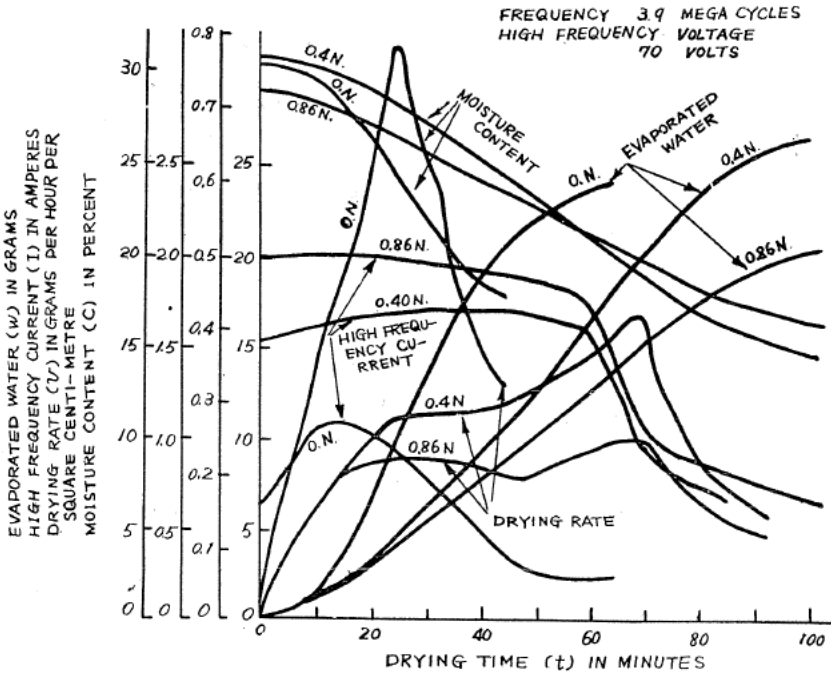

FIG. 8

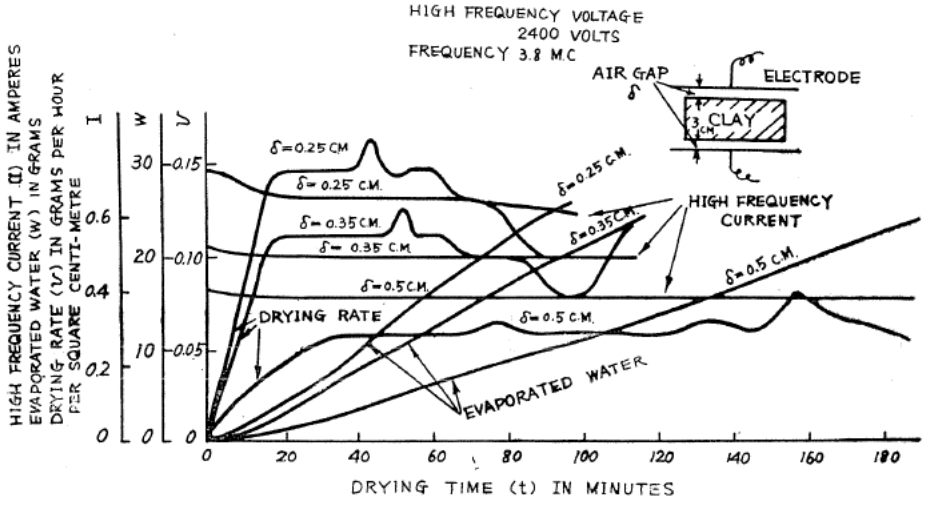

FIG. 9

(3) *On the Grid Electrode.*

When, instead of parallel plate electrodes, a grid electrode was used for drying,

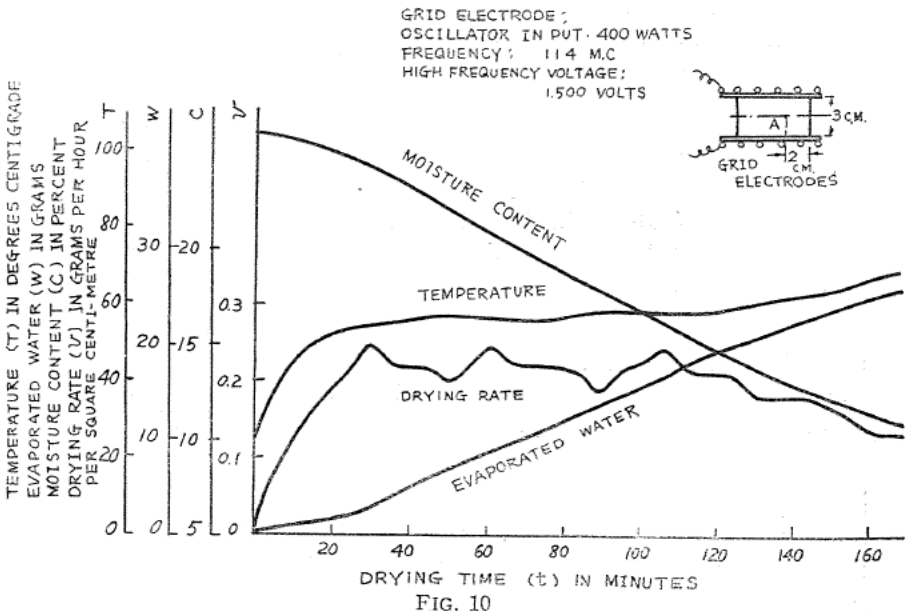

FIG. 10

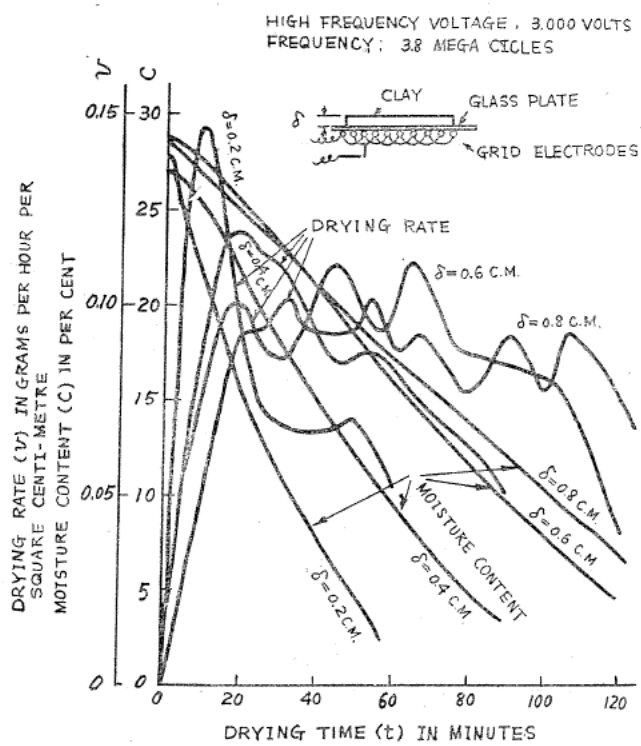

FIG. 11

the results as shown in Fig. 10 and 11 were obtained. Fig. 10 shows the results of the experiment in which the grid electrodes were placed on both sides of the test piece, and Fig. 11 shows those obtained when a grid electrode was placed only on one side of it. (The grid electrode was constructed of copper wires, 0.25 centimeter in diameter and 10 centimeters in length. The spacing between the wires were 1.8 centimeters.) From those results it is found that the grid electrode such as is shown in Fig. 10 is not suitable for drying, because its impedance and the voltage between the electrodes increase, and the transfer efficiency of the electric power becomes smaller. But if a thinner piece is to be dried, the electrode arrangement such as is shown in Fig. 11 has many advantages, for in this arrangement greater drying efficiency is obtained for a very thin test piece, which can be free from any defect that may be produced by the plate electrodes touching with each other.

(4) *On the Coil Electrode.*

If the test piece is placed in the coil and the radio frequency field is applied, drying is effected, as shown in Fig. 12. In this case, the ratio of the diameter (D)

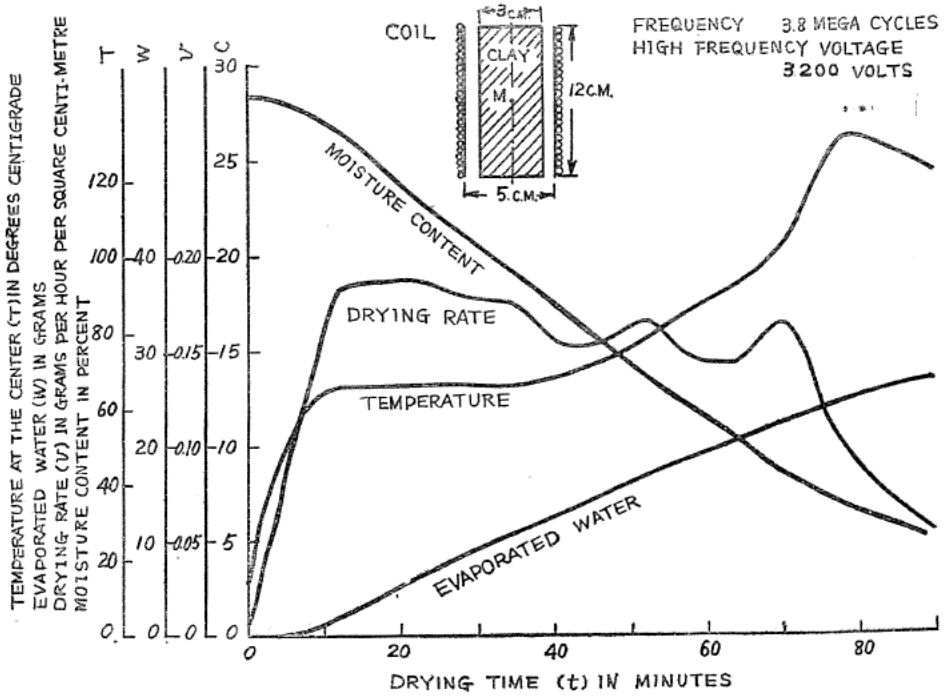

FIG. 12

and the length of the coil must be so selected as to equal the value proper for rapid drying, as shown in Fig. 13. If the clearance between the drying substance and the electrodes is necessary, the coil electrode is more advantageous, because the high frequency resistance of the electrode and the test piece becomes smaller than in other electrode arrangements, as shown in Fig. 14, and the transfer efficiency also becomes greater. But the drying characteristic is not so good and the

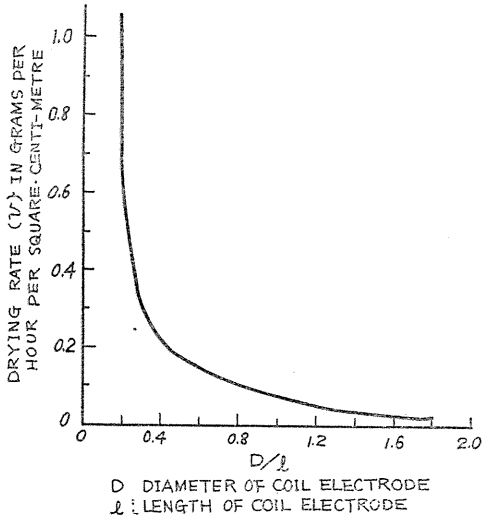

FIG. 13

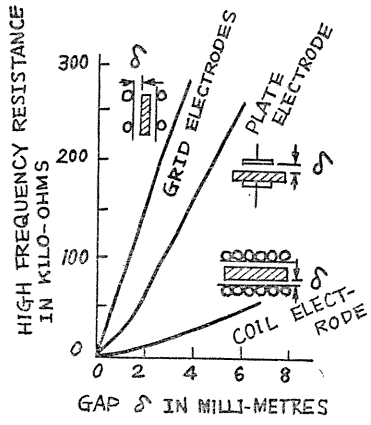

FIG. 14

distribution of the moisture content takes on a paraboric form (Fig. 15). Therefore, if we want to dry any substance uniformly, we should vary the form of the coil electrode or move it gradually through the coil.

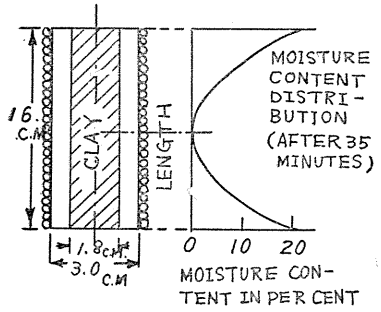

FIG. 15

4. On the Measurement of the Internal Pressure within the Substance.

To explain the drying mechanism of radio-frequency heating and the phenomenon of the "internal explosion," we must examine the internal pressure distribution within the substance at any instant. For this purpose, we inserted one end of a capillary manometer (its diameter being about 1 mm. and its length about 350 mm.) into a desirable position in the substance. Some red alcohol or water was previously poured into the said glass capillary tube, and the other end of it was sealed up in the point flame of a gas-burner. By this method, the internal pressure distribution within the test piece of clay during the drying period was measured, and the result as shown in Fig. 16 has been obtained. (The error due to the expansion of the capillary tube of the manometer has been corrected.) From this result it is found that the internal pressure increases gradually until the end of the constant drying rate period (the range AC in Fig. 16), and then suddenly decreases, falling as low as about one atmospheric pressure (the range CD). When the heating of the test piece was continued, the internal pressure increased again rapidly (range DE), and reached the maximum pressure (E). Next, it decreased gradually till it fell as low down as one atmospheric pressure

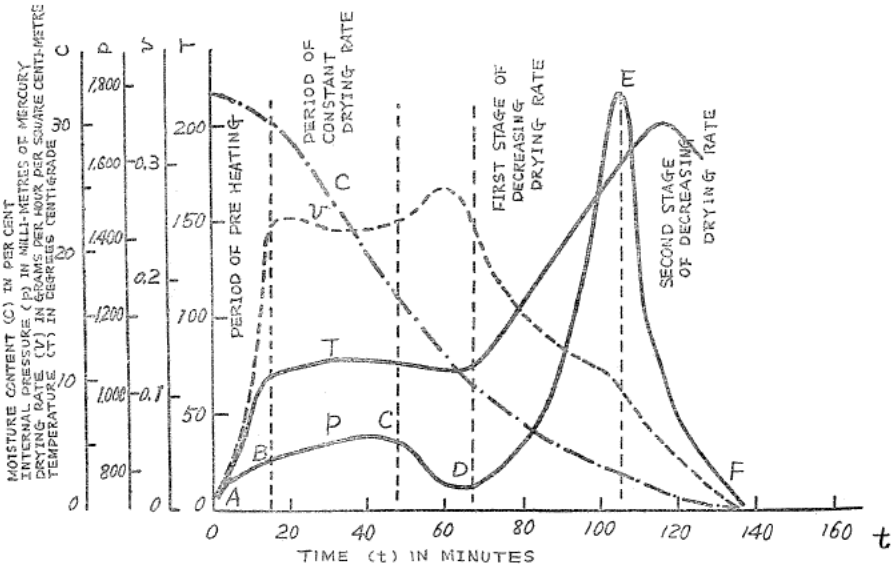

FIG. 16. (Oscillator input, 60 watt; frequency 110 MC.)

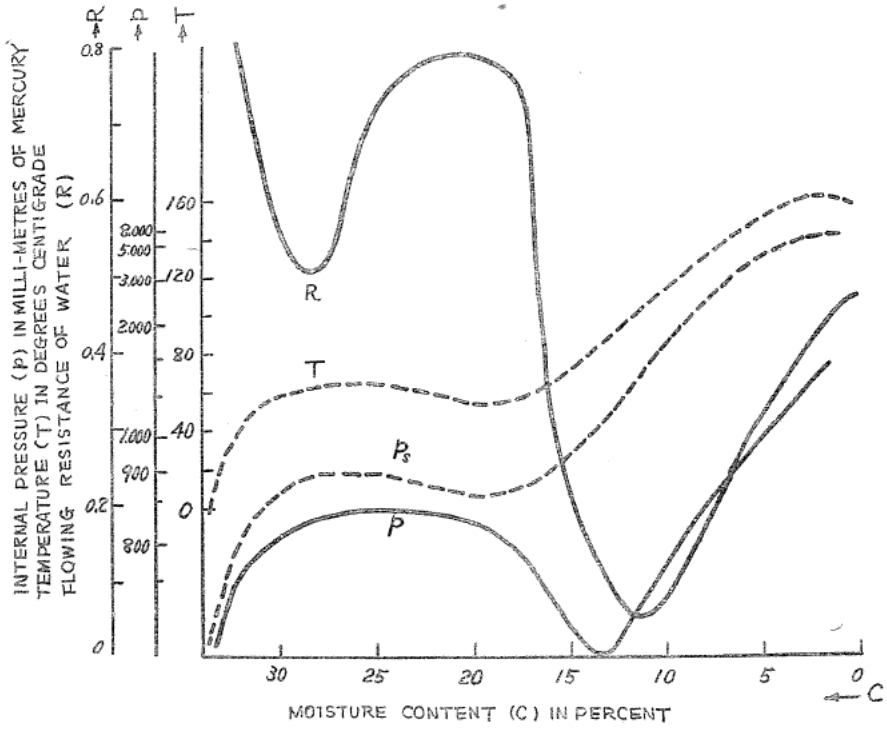

FIG. 17. (Oven-drying with the electric heater of 190 watt.)

(For R and p_s, see on page 22.)

(range F) at the moisture content of zero per cent. In this case, the internal temperature was measured with a thermo-couple of iron-constantan which was inserted in the glass tube with a diameter of about 2 mm., and we obtained the results as shown in Fig. 16. The internal temperature increased simultaneously with the heating, and maintained the contant value for a while and again gradually increased after the period of the decreasing drying rate (range DE). (Sometimes, however, the temperature decreased at the second stage of the decreasing drying rate. This is perhaps due to the fact that the dielectric constant and dielectric power factor gradually decreases as the moisture content decreases.) Similar relations can be obtained in drying by means of oven-heating as shown in Fig. 17. In this case, the internal pressure does not increase so much as in the case of radio-frequency heating, and sometimes the position of the minimum internal pressure distribution (D) moves slightly to the left. This is perhaps due to the fact that the drying is effected insuccesively from the surface of the substance to the center in the case of oven-drying, and the moisture content indicates only the average value of the test piece as a whole, not that of the particular part of it to be measured.

5. The Relation between the Electric Power and the Internal Pressure.

We investigated the relation to be found between the internal pressure and

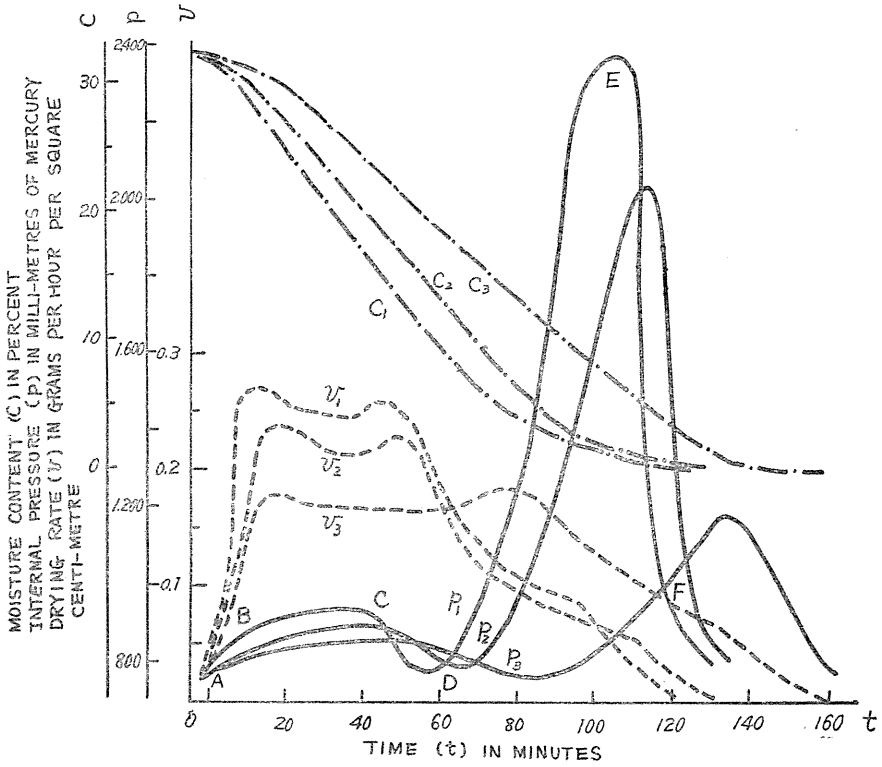

FIG. 18. (Curves for suffix 1: oscillator input, 80 watt. Curves for suffix 2: oscillator input, 65 watt. Curves for suffix 3: oscillator input, 40 watt. Frequeney, 110 MC.)

the electric power when electric powers of 80 Watts, 65 Watts, 40 Watts of 110 MC respectively were transferred into a cylindrical test piece of clay of 33% moisture content, and the results as shown in Fig. 18 were obtained. When the electric power was increased, the increasing rate of the internal pressure together with the numerical value of it was found to increase, while the drying duration was shortened. If the drying rate (v) and the internal pressure (p) are plotted against the moisture content (c), the curve as drawn in Fig. 19 is obtained.

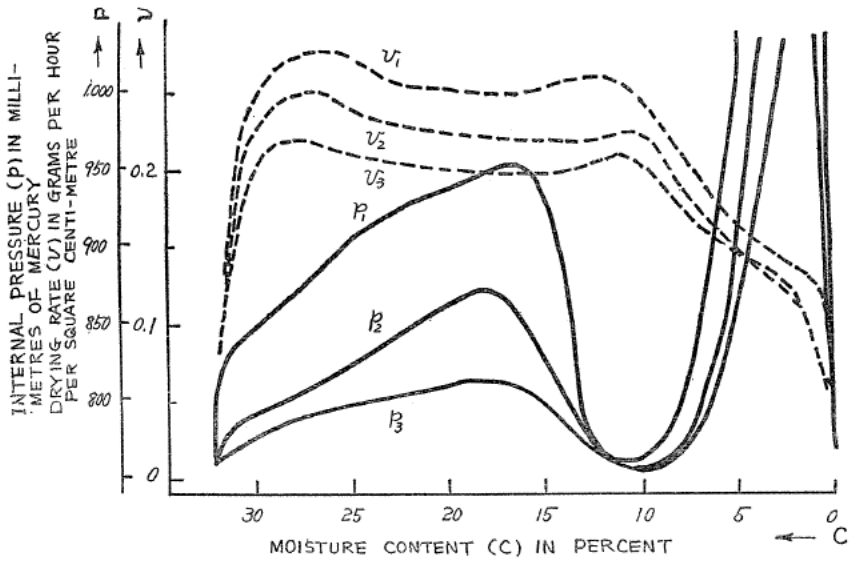

FIG. 19. (*ditto* to Fig. 18.)

It is known, from this curve, that the internal pressure decreases from the moisture content of about 18% and reaches the minimum value at the moisture content of about 10%.

6. The Distribution of Internal Pressure.

In the preceding paragraph we have dealt chiefly with the internal pressure at the center of the substance, but in the present paragraph will be examined the distribution of internal pressure at any point. Fig. 20 and 21 show how intenal pressure is distributed on the xy-plane and xz-plane respectively, when the origin of the co-ordinate system (xyz) conincides with the center of the substance, and as to temperature distribution, we have obtained the same curves on the xy- and xz-plane (see Fig. 22). It must be noted that the above mentioned curves were measured when the electrode and bottom surface of the cylindrical clay test piece were placed in close contact with each other, and the maximum positions of the internal pressure and the internal temperature conincided with the center of the test piece. But, when the electrode was separated to a short distance from the bottom surface of the test piece, the internal pressure distribution became what is shown in Fig. 23 and 24, that is, the maximum position of the internal pressure shifts from the center of the test piece, but the temperature distribution

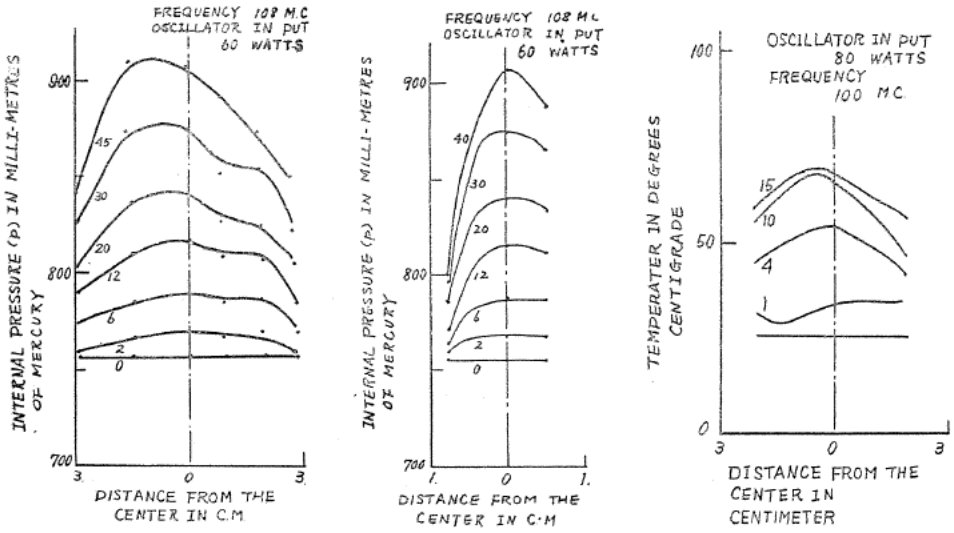

FIG. 20 (*left*). Distribution of the internal pressure on the xy-plane.
FIG. 21 (*middle*). Distribution of the internal pressure on the xz-plane.
FIG. 22 (*right*). Distribution of the temperature on the xy-plane.
(The figures on those curves show the heating time in minute.)

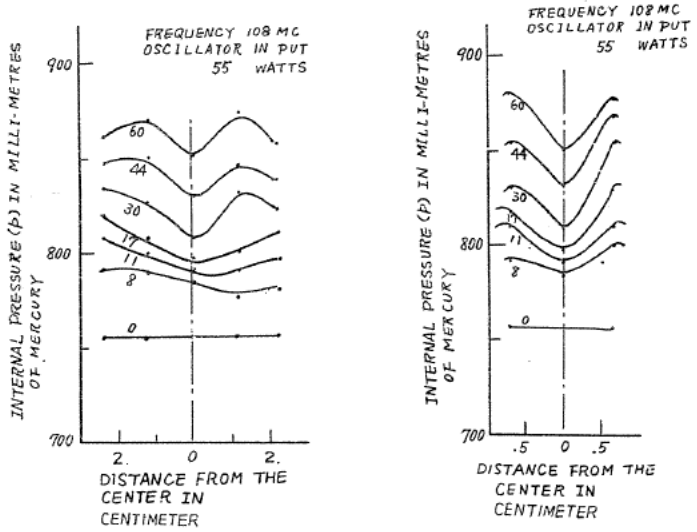

FIG. 23 (*left*). Distribution of the internal pressure on the xy-plane.
FIG. 24 (*right*). Distribution of the internal pressure on the xz-plane.
(The figures on those curves show the heating time in minute.)

does not change its form and conincides with the curve shown in Fig. 22. The cause for this may be that the evaporation in the direction of z-axis is allowed and the length of the test piece in this direction is smaller than that in the direction of x- or y-axis, while the flowing resistance of water in the z-direction becomes smaller, because, if the bottom surfaces of the test piece are covered with glass plates, the internal pressure rises from p_1 to p_2 as shown in Fig. 25.

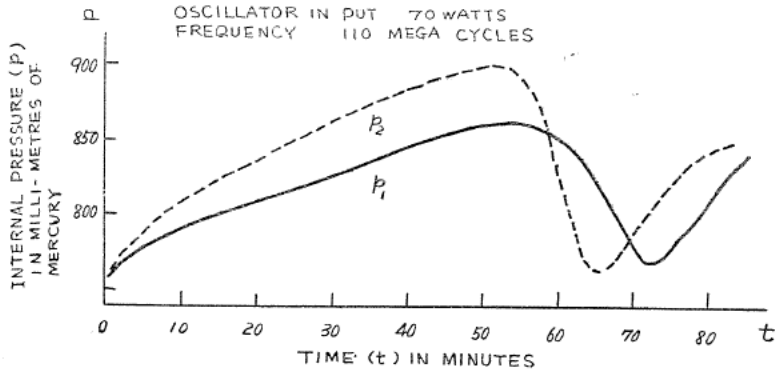

FIG. 25

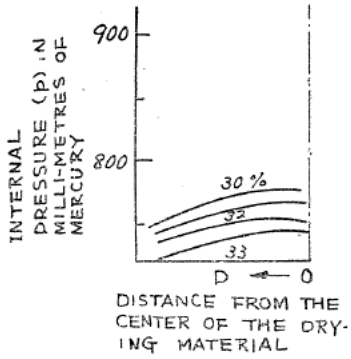

FIG. 26

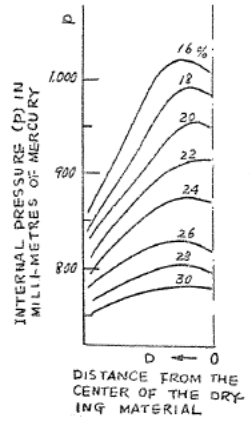

FIG. 27

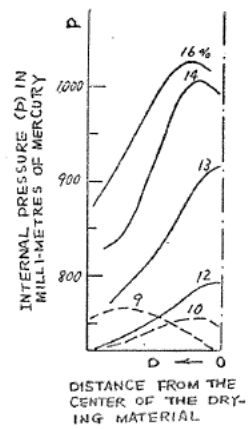

FIG. 28

(Radio-frequency heating, oscillator input 60 watt, frequency 110 MC.)
(The figures on those curves show the moisture content.)

In Figs. 26, 27, 28, 29, 30 and 31 are given the curves indicating the distribution of internal pressure and internal temperature at any instant of the drying period. (The figures on those curves show the percentage of moisture content of the test piece.) Comparing those results with those given in Figs. 16, 20 and 21, we see how internal pressure is distributed at the pre-heating and the constant drying rate period (Figs. 26 and 27), and how it is at the first stage of the decreasing drying rate period (Fig. 28 and 29) and at the second stage of the decreasing drying rate period (Fig. 30). But the temperature of the substance tested, when it is heated, increases gradually as shown in Fig. 31. If this is compared with the shrinkage curve (Fig. 2), it is known that the internal pressure is correlated to the flowing resistance of water or vapor at any instant. Clay is generally considered as uniform material, but in reality it is not; rather it should be considered as a system of capillary paths between grains of clay. Until the constant drying rate period there is liquid free water filling up capillary paths, and when the clay piece is heated internal pressure increases, till it balances with the flowing resistance of water. But the liquid water flows out at the beginning of the decreasing drying period (range *CD* of Fig. 16), and the internal pressure rapidly decreases as

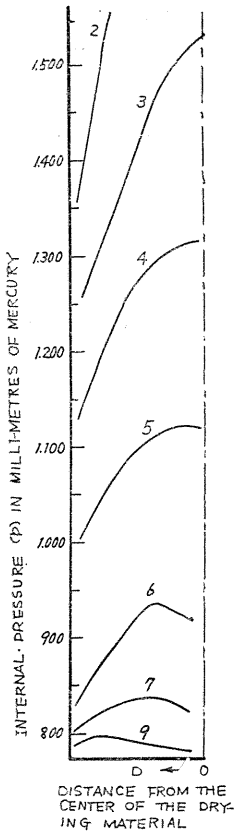

FIG. 29
(Radio-frequency heating.)

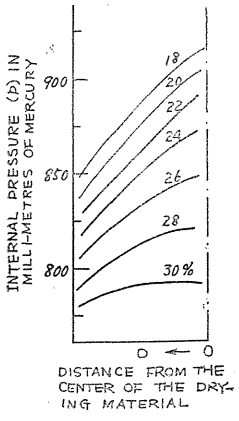

FIG. 32. Oven-drying with electric heater 190 watt.

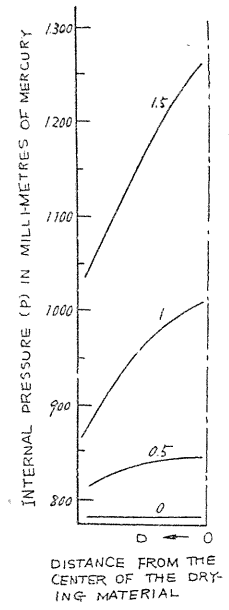

FIG. 30

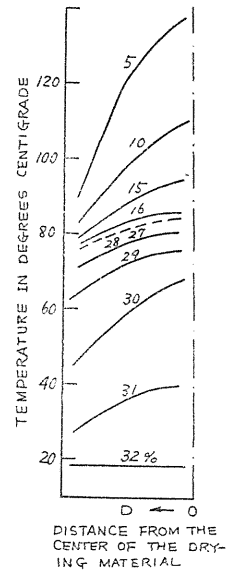

FIG. 31

(Radio-frequency heating.)
(The figures on those curves show the moisture content.)

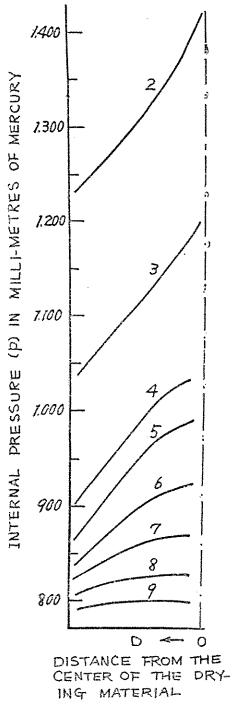

FIG. 33. Oven-drying

shown in Fig. 16 (*CD*). The clay piece shrinks almost to the ultimate state at the moisture content of 10%, the diameter of the capillary paths between grains of clay becomes smaller, and thus the vapor flowing through capillary paths receives greater resistance. Hence, the internal pressure increases as *DE* of Fig. 16 shows. But the amount of water left within the substance to be evaporated becomes so small when the piece is kept on drying, that the internal pressure is no longer allowed to increase and begins to decrease, as shown by *EF* of Fig. 16. Similar relations can be observed in the case of oven-drying as stated above. By measuring the distribution of internal pressure, we obtain the results shown in Figs. 32 and 33. As stated above, internal pressure does not

increase so much as in the case of radio-heating, and the position of the maximum internal pressure always coincides with the center of the substance. The reason for this may be that it is heated from the surface of the substance which is dried and not uniformly by oven-heating. And then, the internal diffusion coefficient of water in the oven-heating is lower than in the case of radio-heating. From these facts it is clear that radio-frequency heating is superior to oven-heating in drying the substance.

7. The Effect of Frequency Variation.

We investigated the effect of the frequency of the applied electric field. In radio-frequency heating, heating is effected by applying the high frequency electrical field; hence, the following equation can be applied:

$$\mathrm{Rot}\,\mathbf{H}=\frac{4\pi}{c}\left(\mathbf{i}+\frac{\partial \mathbf{D}}{\partial t}\right), \tag{5}$$

$$\mathrm{Rot}\,\mathbf{E}=-\frac{1}{c}\frac{\partial \mathbf{B}}{\partial t},$$

where $\mathbf{D}$: electrical displacement
$\mathbf{B}$: magnetic induction
$\mathbf{E}$: electrical field intensity
$\mathbf{H}$: magnetic field intensity
$\mathbf{i}$: conduction current density
c : velocity of light (3×10^{10} cm/sec.)
(Every unit is indicated in C.G.S.)

If these equations are applied to a cylinder, h centimeter high, with the radius of a centimeter, we obtain the following equation.

$$\frac{d^2\mathbf{E}}{dr^2}+\frac{1}{r}\frac{d\mathbf{E}}{dr}+\gamma^2\mathbf{E}=0, \tag{6}$$

where, ε : dielectric constant,
μ : permiability,
f : frequency of the applied electrical field in cycles per second,
r : distance from any point to the center in centimeter.

$$\gamma=\frac{\varepsilon\mu\omega^2-j\,4\pi\sigma\mu\omega}{c^2},\quad \omega=2\pi f.$$

The solution of this equation is

$$\mathbf{E}=AJ_0(\gamma r), \tag{7}$$

where, A : arbitrary constant,
J_0 : a Bessel function of the first and zero order.
Hence, the power per unit volume generated in the substance at any point r cm. apart from the center is[3]

$$P=\sigma E^2=\sigma E_0^2 J_0^2\left(\frac{2\pi r}{\lambda_0}\sqrt{\varepsilon}\right)\quad \text{watts per cubic centimeter,} \tag{8}$$

where, E_0: electric intensity at $r=0$,

and $\lambda_0=\dfrac{3\cdot10^{10}}{f}$.

The total power P_T generated in a cylinder 1 cm. long, with the radius of a cm. is

$$P_T = \int_{r=0}^{r=a} 2\pi r\sigma E^2 dr = \pi a^2 \sigma E_0^2 \left[J_0^2\left(\frac{2\pi a}{\lambda_0}\sqrt{\varepsilon}\right) + J_1^2\left(\frac{2\pi a}{\lambda_0}\sqrt{\varepsilon}\right)\right]. \tag{9}$$

As Dr. G. H. Brown[3] indicates, if we lay down a condition that the power generated per cubic centimeter at the center should not exceed the power density near the surface by more than five per cent, an upper limit on the frequency to be used is given by the relation,

$$f_{MC} = \frac{1482}{a\sqrt{\varepsilon}}, \tag{10}$$

where, a: in centimeter.
Within this limit, the effect of the frequency is scarcely observed except a change in dielectric loss factor ($\varepsilon \tan\delta$). For instance, if the frequency is changed from 75 MC to 150 MC, it becomes what is shown in Fig. 34.

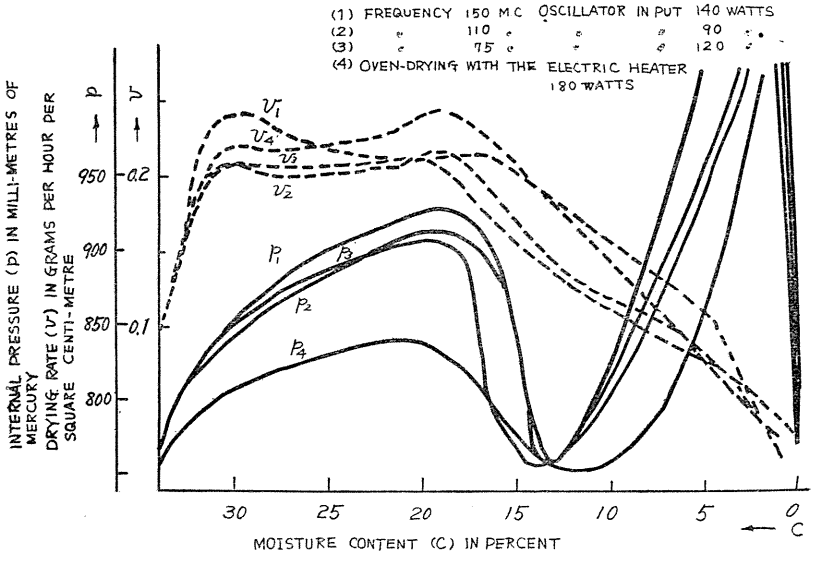

FIG. 34

8. The Relation between the Electric Properties of Clay and its Drying Characteristics.

Since heat is generated, in radio-frequency heating, by the dielectric loss in each molecule, it is necessary to investigate the relation between the eletrical properties and the drying characteristics of clay. In the first place we measured the specific high frequency resistance of clay with the Q-meter and by the differential condenser method, with the results shown in Fig. 35 or Fig. 36. But when we measured the high frequency resistance of clay at any instant of the drying period by the differential condenser method, the results as shown in Fig. 37 were

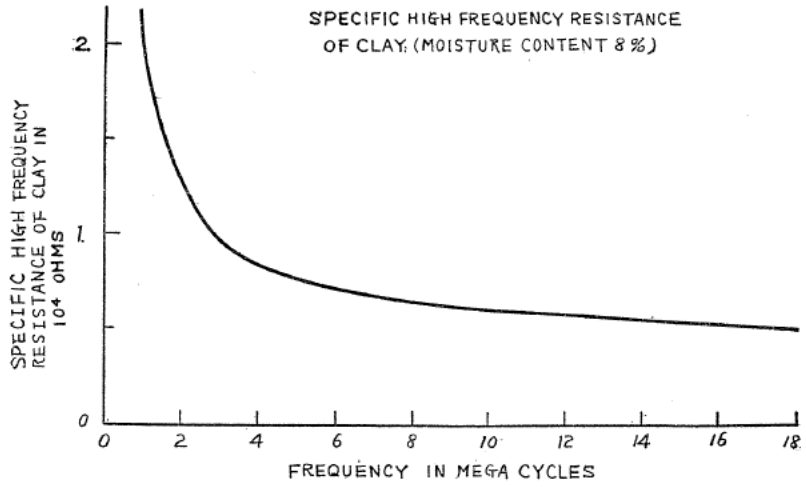

FIG. 35

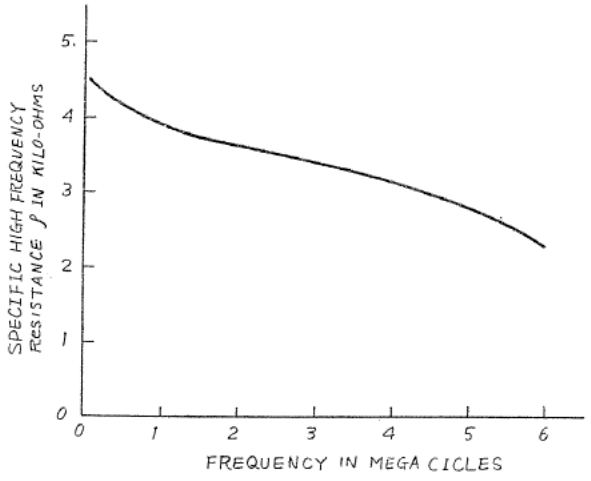

FIG. 36. Specific high frequency resistance of clay (moisture content 25%).

obtained. From this curve, it is found that the curve fluctuates at the moisture content of (10~25%), and rises sharply from the moisture content of 10%. Also, when measurement was made of the dielectric constant of clay, the curve as given in Fig. 38 was obtained. The dielectric constant is seen to become smaller with the decrease in moisture content. When those results above referred to are compared with the fact that the dielectric constant of liquid water is much larger than that of vapor, it will be made clear that all the capillary paths between

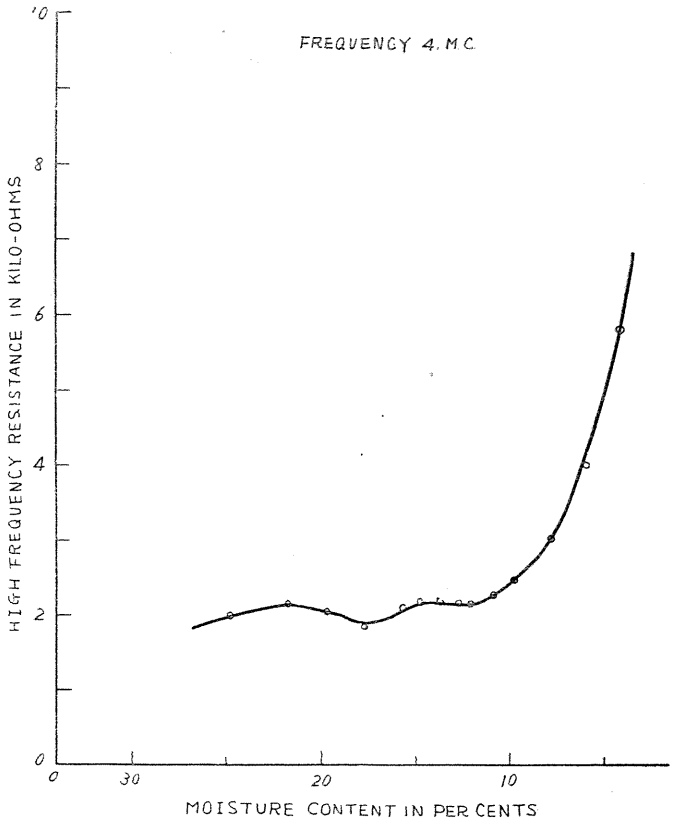

FIG. 37. Variation of the high frequency resistance of clay during the drying period.

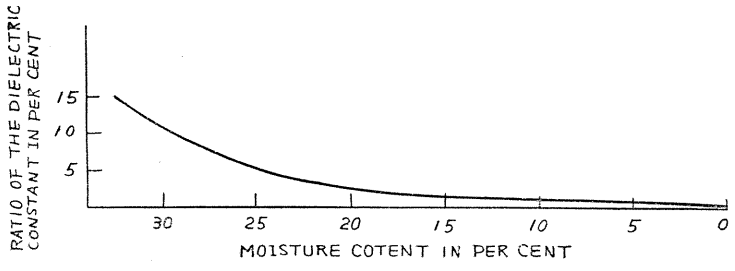

FIG. 38

clay's grains are, when above the critical moisture content, full of liquid water, which flows out successively as the piece is kept on drying, till there is scarcely any liquid water perceptible at the moisture content of 10%.

9. The Effect of the Initial Moisture Content upon Internal Pressure.

As mentioned above, the internal pressure decreases rapidly at the moisture content of about 15%. How will this relation change when the initial percentage of moisture content is changed? In our experiment a piece of clay of initial percentage of moisture content, 33%, 26%, 17%, and 12%, were used and the result

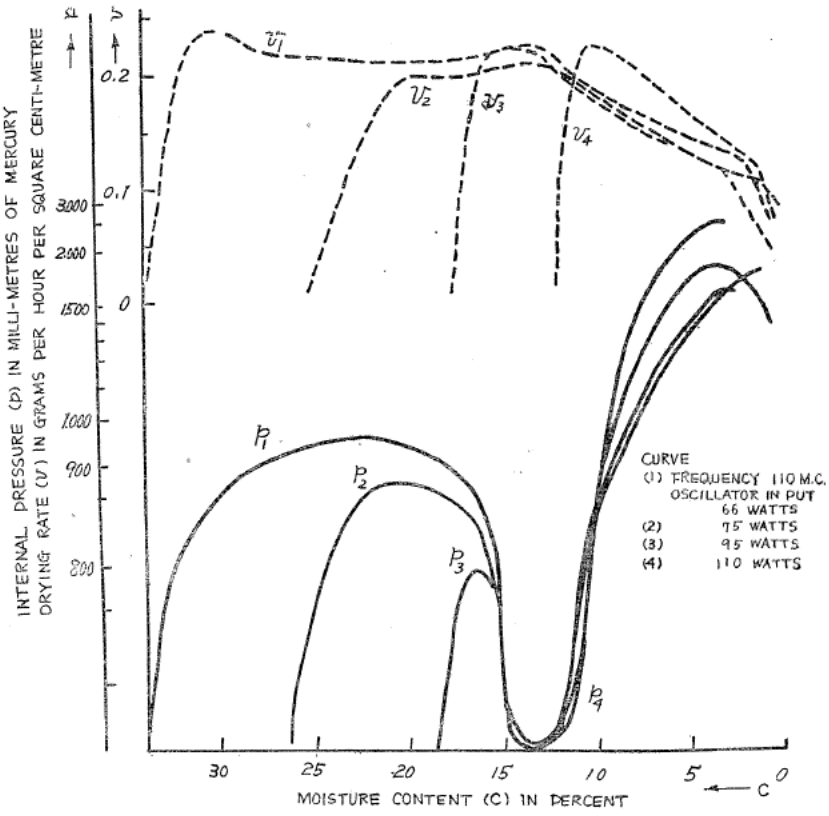

FIG. 39

as shown in Fig. 39 were obtained, which shows that the period of the constant drying rate becomes longer with the increase of the moisture content. And if substance of lower moisture content is heated, the internal pressure distribution curve conincides with the former at the decreasing drying rate period. Hence, the variation of the internal pressure is found to depend upon the physical properties of the substance.

10. The Physical Meaning of the Variation of Internal Pressure.

As stated above, the internal pressure depends upon the physical properties

of substance, especially upon the drying shrinkage. (The drying shrinkage curve of clay is shown in Fig. 2.) Shrinkage begins at the moisture content of about 27% and increases till the moisture content of about 10% is reached, when shrinkage almost ceases. The water contained in the substance consists of free water, semi-bound water and bound water, the liquid free water filling up the capillary paths between grains of clay above the critical moisture content. In this state, if the substance is heated, the internal pressure increases with the increase in temperature until it is balanced with the flowing resistance of the liquid water. The liquid water flows out gradually from the capillary paths mentioned above, and it is almost exhausted at the beginning of the decreasing drying period (*CD* of Fig. 16), but the vapor can easily flow out through the capillary paths. This causes the internal pressure to decrease to about one atmospheric pressure. Clay shrinks when it continues to be dried and almost reaches the ultimate state at the moisture content of 10%, in which state the diameter of the capillary paths referred to above becomes so small as to resist the vapor flowing, causing the internal pressure to increase to the maximum value (*DE* in Fig. 16). According to Poiseuille's equation, the flow of vapor through a capillary tube is given as follows:

$$w_l = \frac{n\pi r^4(p_m - p_0)}{8\eta l}, \tag{11}$$

where, w_l: rate of the flow of vapor,
η: viscosity of vapor (the dynamic coefficient of viscosity of air is 0.1501 cm²/sec. at 0° C and 0.2298 cm²/sec. at 100° C),
n: number of the capillary tubes,
l: length of capillary,
p_m, p_0: pressures at both ends of capillary respectively,
r: average radius of capillary.
(Figures are all in C.G.S. unit.)

If n, $(p_m - p_0)$ and l are the constant, the rate of the flow of vapor is proportional to the fourth power of the radius of capillary, and it decreases rapidly as r decreases. Hence, at the period of *D* of Fig. 16, if the diameter of the capillary tube shrinks slightly, the vapor can not flow out so easily as before described, and the internal pressure increases rapidly and reaches the maximum value. (See the range *DE* of Fig. 16.) If the mechanical strength of substance is smaller than the maximum value of the internal pressure, the "internal explosion" will take place. But, on the contrary, if the mechanical strength of substance is greater than the maximum value of the internal pressure, vapor flows out gradually and the moisture content of the substance decreases. Hence, the internal pressure decreases gradually, reaching ultimately nearly one atmospheric pressure at the moisture content of zero per cent. (See the range *EF* of Fig. 16.)

11. On the Distribution of Moisture Content.

When a test piece of rectangular form (10 cm × 5 cm × 2 cm) was made of clay of 27% moisture content, and the radio-frequency field of 8.2 MC was applied to it, the distribution of the moisture content during period was found to become what is shown in Fig. 40. (This experiment was made in free atmosphere, and

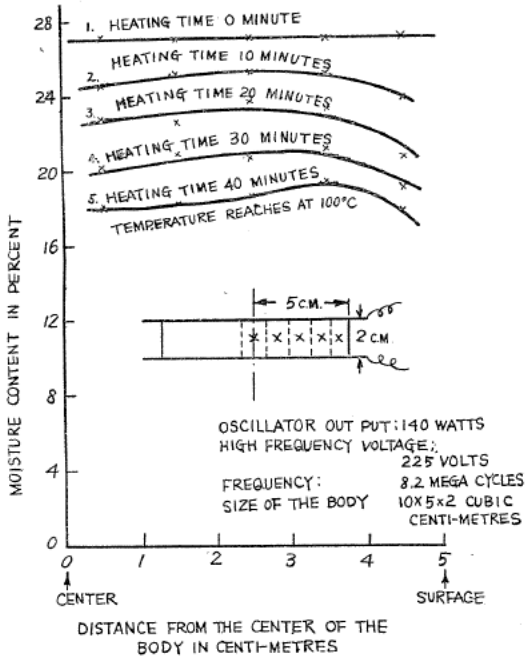

FIG. 40

not in the box described in Fig. 1.) It was found that either the moisture content of the substance tested decreased uniformly, or the flowing-out rate of water was nearly the same at any position. However, as this experiment was made in free atmosphere and the surface evaporation exceeded the internal diffusion of water, the surface was dried and shrank, the flowing-out rate of water decreasing at the surface. Hence, the position of the maximum mositure content was observed between the center and the surface. (See the curve (4) and (5) of Fig. 40.) Therefore, even if the surface is slightly dried, this can be modified by limiting the surface evaporation, and surface cracks can be avoided to some extent in radio-frequency drying. (See Fig. 50 and 51.) (It was noticed, however, that when the electric power transferred into the substance to be dried was too small and the electric potential falls exceedingly at the surface, the inner part of the substance was not heated, and its surface alone was dried.)

12. On the Flowing Resistance of Water.

If the flowing resistance of water be infinitely great, i.e., if the leakage of vapor is zero, the internal pressure must naturally be equal to the saturated vapor pressure at the corresponding temperature of the substance, but if the vapor in the substance escapes out, the internal pressure decreases, hence it can be said that the ratio of the saturated vapor pressure (p_s) and the internal pressure (p) are proportional to the flowing resistance (R) at the moment concerned. That is,

$$R \propto \frac{p-p_0}{p_s-p_{s0}}, \tag{12}$$

where, p and p_s denote the respective pressure at any instant, and p_0 and p_{s0} the respective pressure at the initial state.

The results calculated from the above experimental data are given in Fig. 41. This flowing resistance curve nearly coincides with that of the internal pressure,

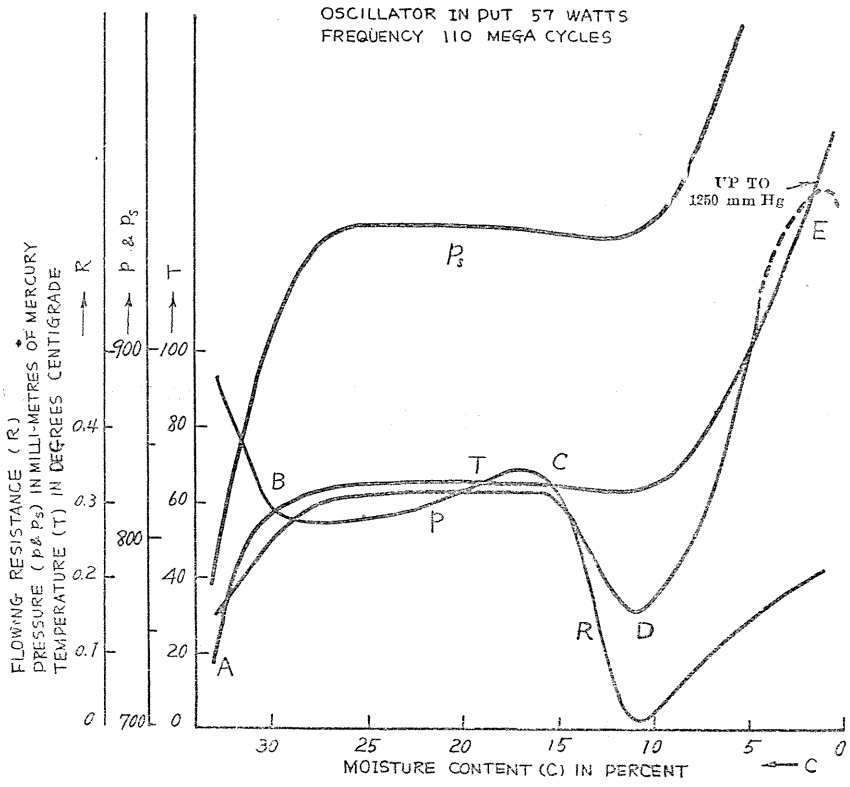

FIG. 41

except at the pre-heating period. In other words, the decrease in the flowing resistance R when heating is begun, is perhaps due to the decrease in the surface tension of water and the modification of the degree of dryness of the surface of substance when temperature is kept on increasing. What is stated above is confirmed by the result given in Fig. 42, which shows the relations between the flowing resistance at the time of intermittent heating and cooling respectively. As for the relation between the drying rate and the flowing resistance of water, see Fig. 43. If the drying rate is increased, the flowing resistance decreases, the "internal explosion" taking place in the portion between the dotted lines. Compare with this, the flowing resistance in the case of oven-heating, which is shown in Fig. 17, is larger than that seen in the case of radio-frequency heating. From this fact, we are led to conclude that radio-frequency drying is better than oven-drying for drying substance.

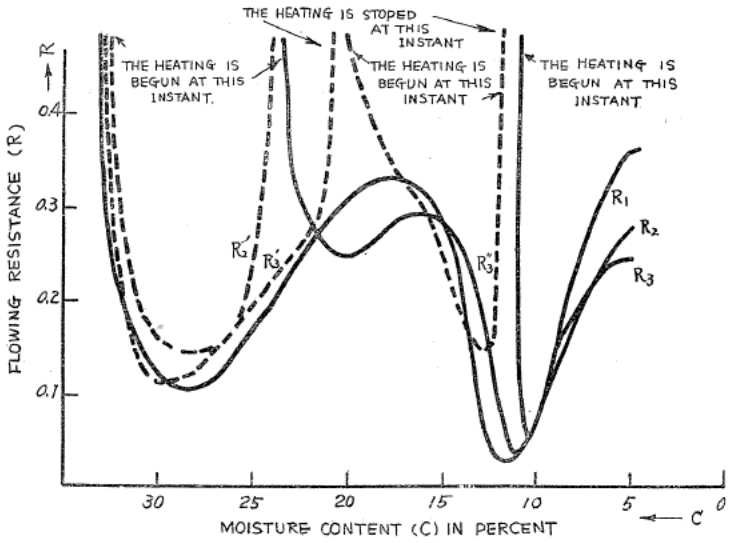

FIG. 42. (R_1: oscillator input, 60 watt. R_2 and R_2': oscillator input, 70 watt. R_3, R_3' and R_3'': oscillator input, 85 watt. Frequency, 110 MC.)

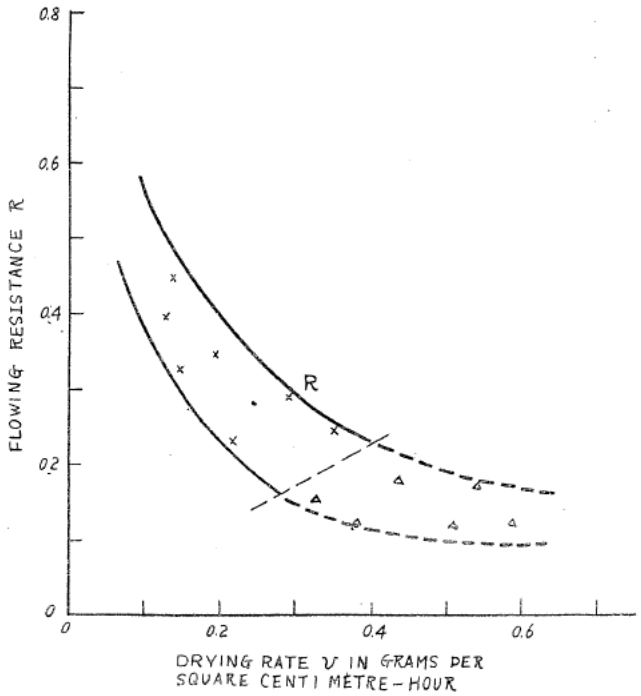

FIG. 43

13. The Internal Pressure within Wood.

A slender hole was bored previously in a piece of wood, and one end of the capillary manometer mentioned above was inserted into it, and the small space left in the hole was air-tighted with phenol-resin. In this way we measured the internal pressure at any instant during the heating period.

(*1*) *Japanese Cypress.*

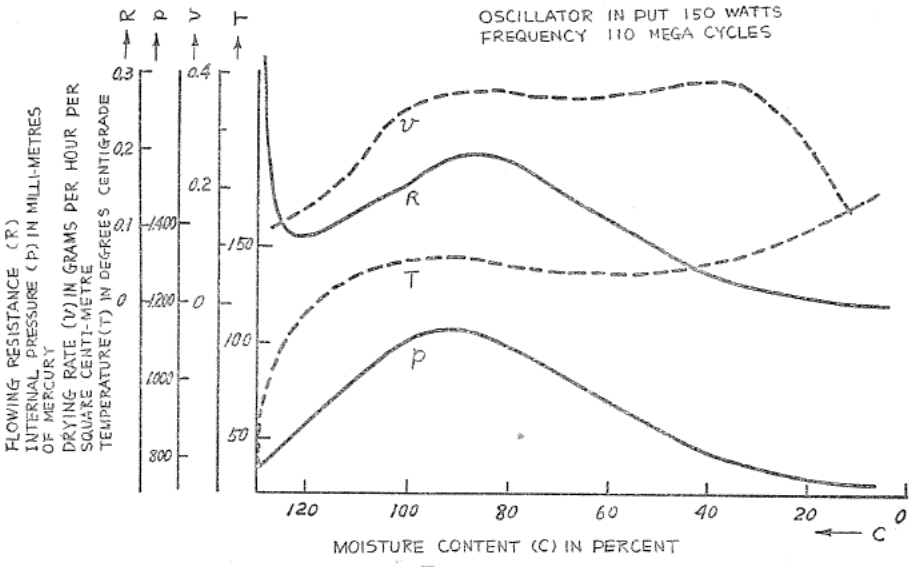

FIG. 44

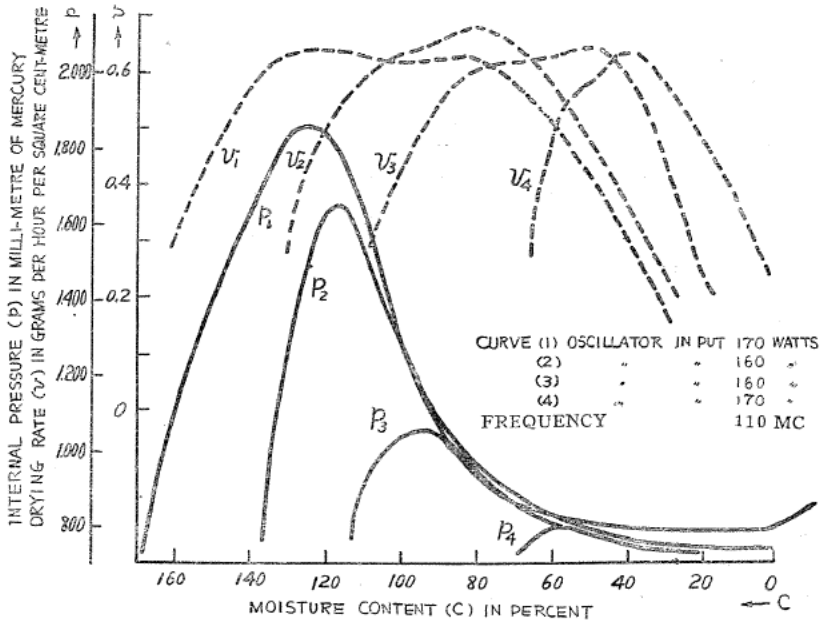

FIG. 45

When the high frequency field of 110 MC was applied to the test pieces (5 cm × 5 cm × 2 cm) of Japanese cypress with moisture content of 20%, 70%, 115%, 137% and 170%, the results as shown in Fig. 44 and Fig. 45 were obtained respectively. When a capillary manometer was inserted into the test piece perpendicularly to the radial section (Fig. 46) and the distribution of the internal pressure along wood fiber (y-direction of Fig. 46) was measured, the expriment resulted in a smooth curve such as is shown in Fig. 44, but the distribution of internal pressure in a perpendicular direction to that of wood fiber (x-direction of Fig. 46) was too irregular to describe any curve whatever. Hence, it is known that water flows out mainly in the direction along wood fiber, but the diffusion of water in perpendicular direction to wood fiber seldom occurs. From Figs. 44 and 45 it is found that the distribution curve of internal pressure in this case has only one maximum point, and differs widely from that of clay (see Fig. 16). This is perhaps due to the fact that the diameter of a coarse capillary tube such as tracheids or vesselsegments of wood is greater than the clearance between clay's grains, and consequently, while the water flowing out receives some resistance, the vapor meets with far less resistance at any time. In general, wood mainly consists of cells, and the space between these is filled up with liquid water until the fiber saturation point is reached, and water flows out as the piece goes on drying. Here, attention must be called to this, that the experimental results in the present case show, not the internal pressure between cells, but only the internal pressure of coarse capillary systems snch as tracheids or vesselsegments; for, the capillary manometer used in these experiments, which has a diameter of about 1 mm. can indicate the latter alone. According to Poiseuille's equation mentioned above, the internal pressure between cell walls is much larger than that of coarse capillary systems such as tracheids or vesselsegment. Now, in order to study the phenomenon of "internal explosion" of wood, the internal pressure between cell walls must be examined; but since it is impossible to measure this, we must decide the safety factor by which the internal pressure of coarse capillary systems is to be multiplied. This safety factor may be found if we measure the average diameter of tracheids or vesselsegments of wood, together with the clearance between cell walls. The clearance between cell walls is, according to J. Duclaux and J. Errera,[4] about $(0.3\sim30)\times10^{-7}$ centimeters, and the average diameter of tracheids or vesselsegments of wood can be roughly measured with a microscope. But the following consideration of this relation has been made from another view-point. When wood is dried by radio-frequency heating, the "internal explosion" may take place, and the internal pressure in this case must exceed the mechanical strength of wood. If we assume the mechanical strength of Japanese Cypress as (30~60) kilograms per square centimeter, the internal pressure in this case must be the same as the vapor pressure at the temperature about (232.8~274.3) degrees Centigrade or higher. But the experimental results (Fig. 45) show that the maximum internal pressure is about 2.4 kilograms per

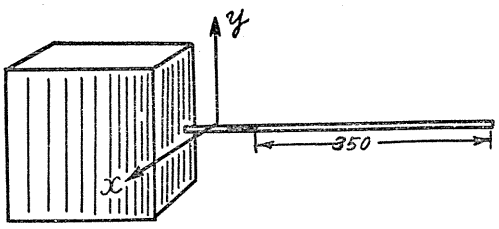

FIG. 46

square centimeter, and it is equal to the saturated vapor pressure at 125° C. If we note that the rise in the internal pressure at the moisture content of zero per cent (Fig. 45) is due to the smoke of wood burning, the internal temperature of wood must be 232.8° C. or more when "internal explosion" takes place. From this it follows that the internal pressure between cell walls must be much larger than that of tracheids or vessel-segments of wood. If the drying rate of Japanese Cypress is raised to 0.8 grams per hour per square centimeter, the "internal explosion" will take place at last. Therefore, we must never allow the drying rate to exceed the rate above referred to. Figs. 47 and 48 show microscopic pictures of green wood (Japanese Cypress) and dried wood respectively. In these pictures we can scarcely find any difference between them. Next, if Japanese Cypress is dried by oven-heating, the curve as given in Fig. 49 is traced. The

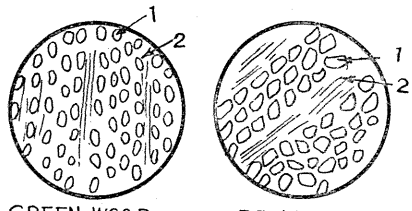

GREEN WOOD
1. VESSEL SEGMENT
2. ANNUAL RING

FIG. 47

DRYED WOOD
1. VESSEL SEGMENT
2 ANNUAL RING

FIG. 48

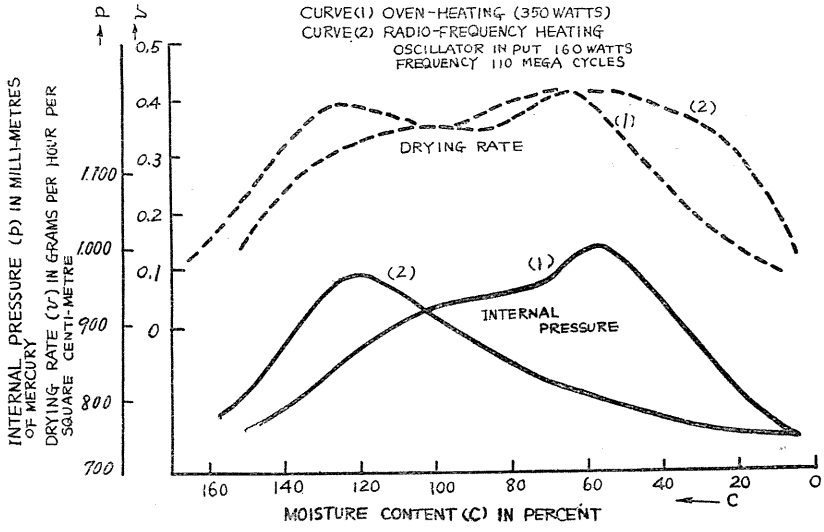

FIG. 49

internal pressure in this case shifts considerably to the right, and the curve is not so smooth as in the case of radio-frequency heating. This may mean that in the case of wood, it is not dried uniformly by oven-drying, but its surface is mainly dried. Hence the surface may easily crack. The distribution of moisture content when Japanese Cypress is being dried describes such a curve as is given in Fig. 50, and the moisture gradient at the surface in this case was observed to increase greatly with the increase in the drying rate. But when it was dried by radio-frequency heating, the distribution curve became what Fig. 51 shows. This means that the moisture gradient at the surface is small and the surface crack does not so readily

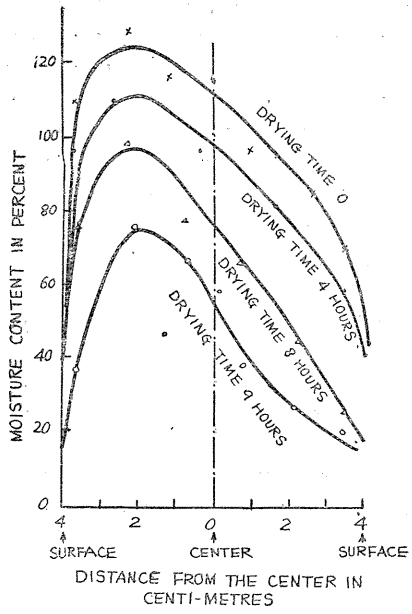

FIG. 50

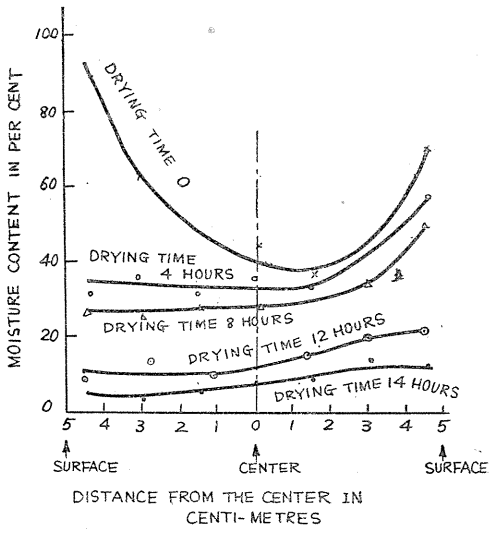

FIG. 51

form as in the case of oven-drying, if the surface evaporation is properly limited.

(2) *Japanese Cedar.*

The result obtained when Japanese Cedar is dried (see Fig. 52) is very similar to that seen in the case of Cypress, but the allowable drying rate is higher

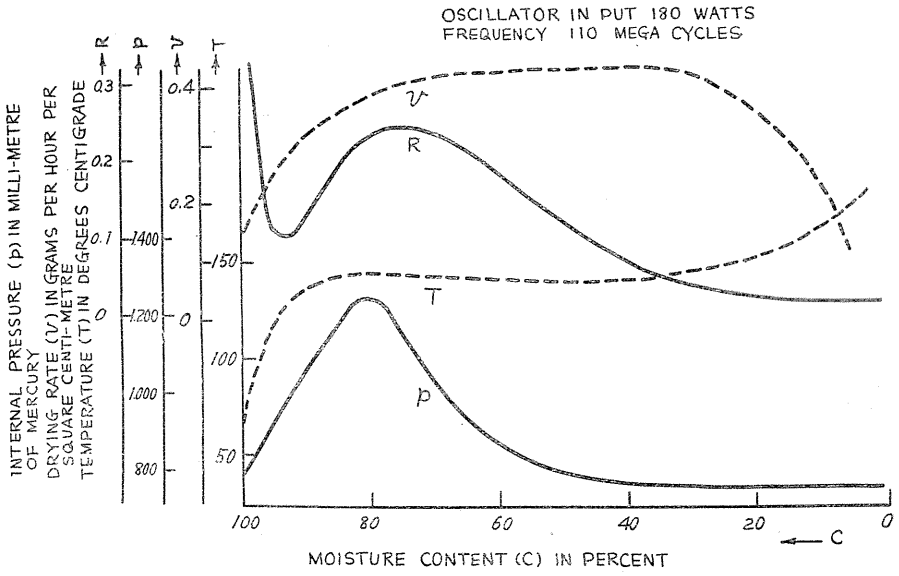

FIG. 52

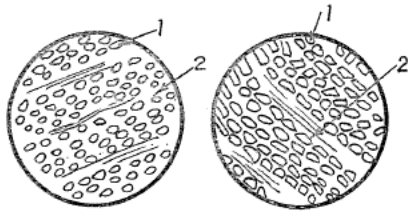

FIG. 53

FIG. 54

than in the case of the latter, the drying rate for practical purpose being at 0.8 grams per hour per square centimeter. The microscopic pictures of Japanese Cedar are given in Figs. 53 and 54. Fig. 53 being that of green wood and Fig. 54 of dried wood. Also in these pictures, we can scarcely find any difference between them.

(3) *Beech Tree.*

Fig. 55 shows the results of an our expriment with the Beech tree. This

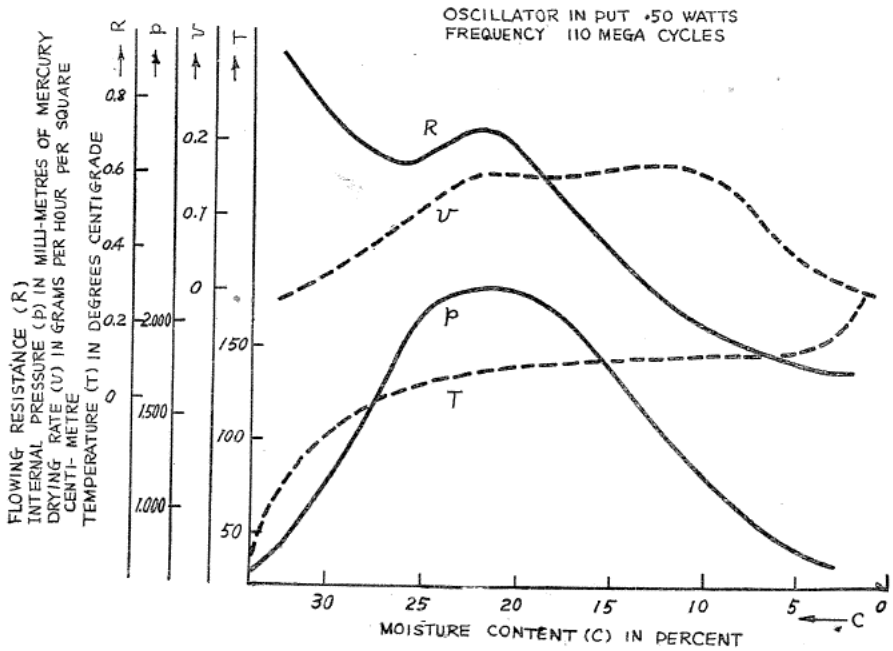

FIG. 55

experiment has shown that the internal pressure and the drying rate is smaller than in the case of Cypress; how these change with the changes in the electric power is shown in Fig. 56. Fig. 57 and Fig. 58 show a microscopic picture of

green wood and of dried wood respectivey.

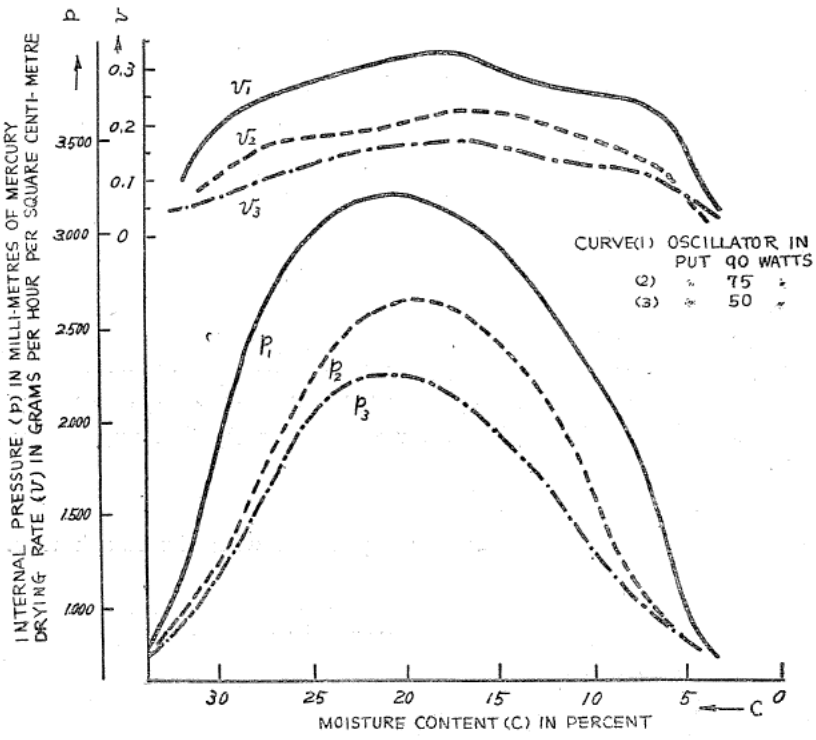

FIG. 56

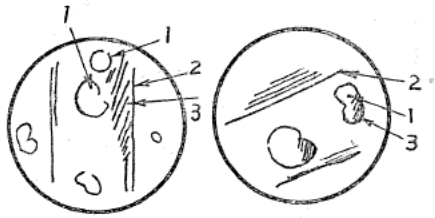

FIG. 57

FIG. 58

(4) *Cercidiphylum Japonicum.*

Fig. 59 shows the result of our experiment with *Cercidiphylum Japonicum.* This result is very similar to that of the experiment with Cypress, but, in the present case, when the electric power is increased, the internal pressure does not increase as was the case with Cypress. This is attributable to the crack forming along the annualring, which can be seen from the microspic picture given in Fig. 61. (Fig. 60 is a picture of green wood and Fig. 61 represents dried wood.) It is

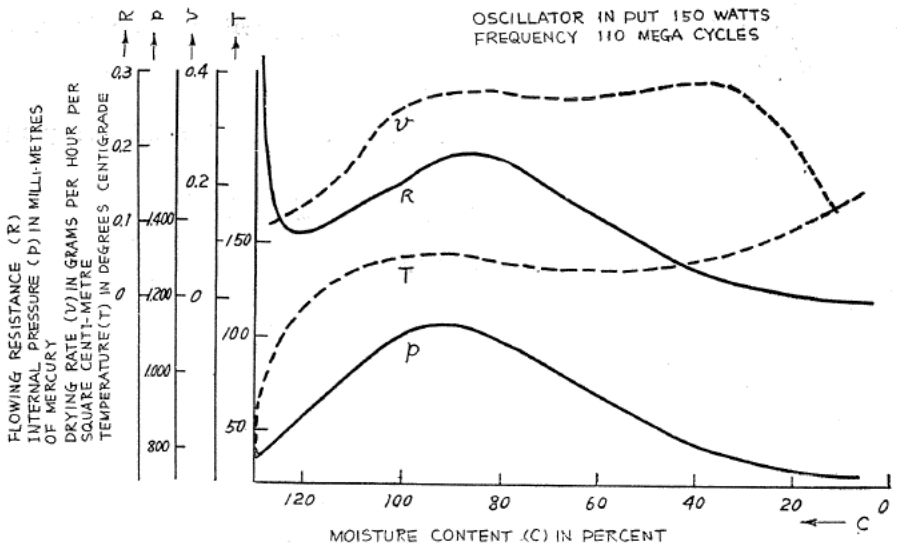

FIG. 59

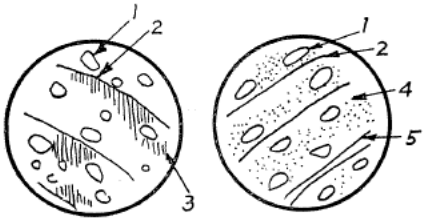

1. TRACHEIDS
2. ANNUAL RING
3. RESIN

FIG. 60

1. TRACHEIDS
2. ANNUAL RING
4. SMALL HOLE
5. CRACK

FIG. 61

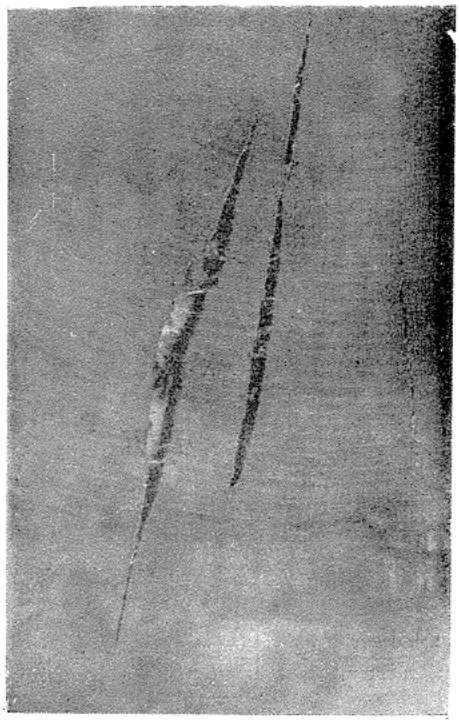

FIG. 62

found that if *Cercidiphylum Japonicum* is heated, the tracheids are enlarged and a crack may develop along the annualring, or the pith line, as shown in Fig. 62. This may mean that the "internal explosion" takes place near the annualring or

the pith line, and so we must dry *Cercidiphylum Japonicum* with lower electric power density.

(5) *Oak.*

Fig. 63 is the result of our experiment on oak. Fig. 64 is a microscopic picture

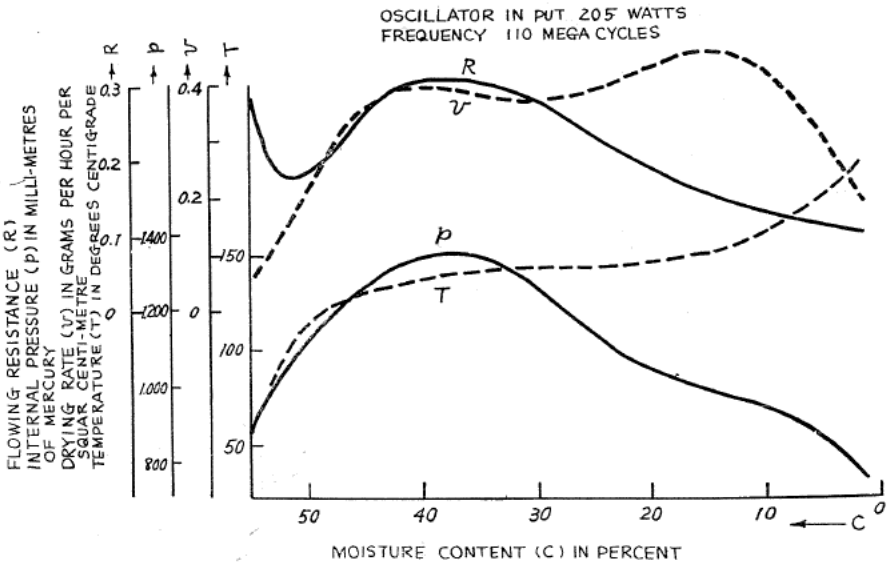

FIG. 63

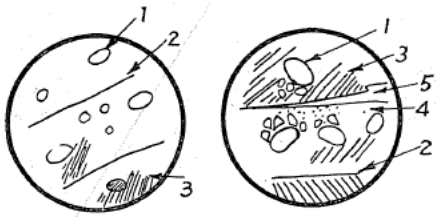

FIG. 64

FIG. 65

of green wood and Fig. 65 is that of dried wood. Those results are similar to those obtained in the case of *Cercidiphylum Japonicum.*

(6) *Camphor Wood.*

The result obtained in the case of Camphor wood is given in Fig. 66. Fig. 67 being a microscopic pic-

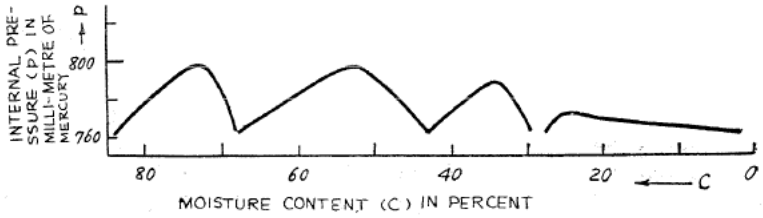

FIG. 66

ture of green wood and Fig. 68 being that of dried wood. The curve in Fig. 66 is very curious, but it is due merely to the cracks caused along the annualring, which appear successively along the annualring in the case of Camphor wood.

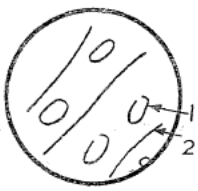

1. VESSEL SEGMENT
2. ANNUAL RING

FIG. 67

1. VESSEL SEGMENT
5. CRACK

FIG. 68

14. On the Drying Mechanism of Radio-Frequency Heating.

Up to this time, the drying mechanism of clay has been attributed to the internal diffusion and the surface evaporation of water, and this has been explained by means of the following equation:

$$\frac{\partial c}{\partial t} = D\left(\frac{\partial^2 c}{\partial x^2} + \frac{\partial^2 c}{\partial y^2} + \frac{\partial^2 c}{\partial z^2}\right) \tag{13}$$

where, c : concentration of water,
D: diffusion coefficient,
x, y, z: co-ordinate axis,
t : time.

If clay be assumed as uniform material, the above equation may be justly employed for such explanation, but the experimental results described above are infavorable to such assumption; clay should be considered rather as a capillary system, and upon this should be based our discussion of the drying mechanism of clay, wood, textiles, etc. The flowing rate of water or vapor can be calculated from Poiseuille's equation for the flow of liquld through the capillary system under pressure.

$$w_l = \frac{n\pi \cdot r^4}{8\eta l}(p_{max} - p_s) \tag{14}$$

where, w_l: rate of the flow of water or vapor,
η : viscosity of water or vapor,
r : average radius of capillaries,
l : length of the capillary,
n : number of the capillary,
p_{max}: maximum internal pressure at the center of the drying substance,
p_s: vapor pressure at the surface of the drying substance.
(Figures are all in C. G. S. unit.)

If n, r, l and η are known from the structure of substance and from other experiments, the flowing rate (w_l) can be calculated from the difference between the maximum internal pressure (p_{max}) and the surface pressure (p_s). In this state, if an element of volume in the capillary system be assumed, the amount of water within it may be measured by finding the excess of water which comes out of it over that which goes into it, and the amount of water evaporated from its inner

surface, and in this way we obtain the following relations:

$$w=-\lambda\left(\frac{\partial^2 p}{\partial x^2}\right), \tag{15}$$

where, w: the amount of water per unit volume per unit time,
λ : a constant, depending on the diffusion coefficient etc..
Therefore,

$$p=-\frac{w}{2\lambda}x^2+C_1x+C_2, \tag{16}$$

where, C_1 and C_2 are integration constants. If the origin of the co-ordinate system coincides with the center of the substance, and substitute in this equation the following two relations.

1) The maximum internal pressure appears at the center of the substance, that is,

$$p=p_{max} \quad \text{at} \quad x=0. \tag{17}$$

2) As stated above (see equation (10)), the frequency to be employed in radio-frequency heating is

$$f=\frac{1482}{a\sqrt{\varepsilon}}\times 10^6 \quad \text{cycles per second,} \tag{18}$$

where, $2a$: dimension of substance to be dried,
ε : dielectric constant of it.
Hence, the temperature at the distance of $\frac{3\cdot 10^{10}}{4f}\fallingdotseq 5a\sqrt{\varepsilon}$ cm. from the center of the substance is zero. If we assume the saturated vapor pressure at zero degree Centigrade to be zero,

$$p_{max}=\frac{w}{2\lambda}(5a\sqrt{\varepsilon})^2. \tag{19}$$

In drying the substance, the maximum internal pressure (p_{max}), as mentioned above, must be lower than its mechanical strength, whence the allowable maximum internal pressure can be found. Next, we shall consider the allowable temperature rise and the surface temperature and pressure p_s.

15. On the Allowable Temperature Rise in Radio-Frequency Heating.

The allowable temperature rise can be found from the allowable internal pressure from the following relation[5].

$$\log\left(\frac{p_c}{p}\right)=F(\Theta)\frac{\Theta_c-\Theta}{\Theta}. \tag{20}$$

Where, p_c: critical vapor pressure in kilogram per square centimeter,
Θ_c: critical temperature in absolute unit,
Θ : temperature of the saturated vapor in absolute unit,

p: saturated vapor pressure in kilogram per square centimeter,
$F(\Theta)$: a function of temperature.

For instance,

$$F(\Theta) = \{7.21523 + (\Theta - 483.2)^2/(\alpha + \beta\Theta^n)\} \tag{21}$$

$$\alpha = 85000, \quad \beta = 46.0, \quad n = 1 \text{ for } 273 \leqq \Theta \leqq 483^\circ \text{ K}.$$

We shall next discuss the temperature rise of the substance in order to find the allowable electric power density in the case of radio-frequency drying and the capacity of the high frequency source. Let us suppose the electric power per unit volume of the substance to be P, then the heat to be generated per unit time will be

$$H = JP, \tag{22}$$

where, J is a constnt.

If an element of volume dV of the substance be assumed, the heat quantity Q_0 to be generated within it is

$$Q_0 = H \cdot dV \cdot dt, \tag{23}$$

where, t: time.

This heat quantity must be balanced with the following three kinds of losses under the steady condition. The said losses are:

1) the heat quantity due to the temperature rise of substance

$$Q_1 = s \cdot \rho \frac{\partial \theta}{\partial t} \cdot dV \cdot dt, \tag{24}$$

where θ denotes temperature, s the specific heat, and ρ the density of substance,

2) the heat loss due to conduction

$$Q_2 = -k \frac{\partial^2 \theta}{\partial x^2} \cdot dV \cdot dt, \tag{25}$$

where, k denotes heat conductivity,

3) the heat loss through the evaporation of water

$$Q_3 = w_l \cdot H_w \cdot dV \cdot dt, \tag{26}$$

where w_l denotes the amount of liquid water evaporated per unit volume per unit time, and H_w the latent heat of evaporation.

From those relations, we obtain

$$(H - w_l \cdot H_w) = s \cdot \rho \cdot \frac{\partial \theta}{\partial t} - k \frac{\partial^2 \theta}{\partial x^2}. \tag{27}$$

Under the steady condition, $\frac{\partial \theta}{\partial t} = 0$, and

$$-k \frac{\partial^2 \theta}{\partial x^2} = (H - w_l \cdot H_w). \tag{28}$$

Solve this equation,

$$\theta = \frac{(w_l \cdot H_w - H)}{2k} x^2 + C_1 x + C_2 \tag{29}$$

where C_1 and C_2 are integration constants.
If the origin of the coordinate system coincides with the center of the substance, and substitute in this equation the following two conditions; i.e.

1) $\theta = \theta_{max}$ at $x = 0$,
2) as described above (see the equation (18)), when the substance is very large, temperature at the position $x \fallingdotseq 5a\sqrt{\varepsilon}$ cm. becomes to zero.

Then, we obtain

$$\theta_{max} = \frac{(H - w_l \cdot H_w)}{2k}(5a\sqrt{\varepsilon})^2, \tag{30}$$

and

$$\theta = \frac{(H - w_l \cdot H_w)}{2k}\{(5a\sqrt{\varepsilon})^2 - x^2\}. \tag{31}$$

16. On the Allowable Electric Power Density.

From the equation (30) the heat quantity H at the maximum temperature can be calculated.

$$H = w_l H_w + \frac{2k\theta_{max}}{(5a\sqrt{\varepsilon})^2}. \tag{32}$$

Substitute the equation (14) in it

$$H = \frac{n\pi r^4 H_w}{8\eta l}(p_{max} - p_s) + \frac{2k\theta_{max}}{(5a\sqrt{\varepsilon})^2}. \tag{33}$$

If the relation between the vapor pressure p and the temperature θ in the equation (20) is assumed as follows,

$$\log \frac{1}{p} = \frac{1}{K}\theta$$

where, K: proportional constsnt.
The electric power density P in radio-frequency drying is

$$P = \left\{\frac{n\pi r^4 H_w}{8\eta l}(p_{max} - p_s) + \frac{2kK \log(1/p_{max})}{(5a\sqrt{\varepsilon})^2}\right\} \times 4.18$$

watts in cubic centimeter. (34)

If H is 599 calories,

$$P = \left\{982.5\frac{nr^4}{\eta l} \cdot (p_{max} - p_s) + 0.3\frac{kK}{a^2\varepsilon} \log \frac{1}{p_{max}}\right\}$$

watts in cubic centimeter. (35)

As stated above, if the maximum internal pressure p_{max} is limited within the allowable value from the mechanical strength of substance, the allowable electric power density (P) in radio-frequency drying can be calculated from the above

equation. If the volume of the drying substance is known, the capacity of the radio-frequency oscillator to be used can also be determined. Let the heat conductivity of wood be given as k.[6]

$$\left.\begin{aligned} k &= g(1.39 + 0.028\,c) + 0.165 \\ &\quad \text{for moisture content } c < 40\%, \end{aligned}\right\} \quad (36)$$

and

$$\begin{aligned} k &= g(1.39 + 0.038\,c) + 0.165 \\ &\quad \text{for } c > 40\%, \end{aligned}$$

(where, g denotes specific gravity of wood.)

and the number of capillaries per square centimeter (n) is $(4 \sim 8) \times 10^5$, the radius of the capillary of wood (r) is 10^{-6} cm., viscocity of water (η) is 0.02 cm²/sec. at 0° C. and 0.003 cm²/sec. at 100° C., and the mechanical strength of wood is (30~60) kg/cm.² When the dielectric constant (ε) and power factor ($\tan\delta$) during the drying period are measured with a Q-meter or by the differential condenser method, the results shown in Figs. from 69 to 73 are obtained. If length of the capillary (l) is equal to the size of the drying wood (a), the allowable electric power density in radio-frequency drying becomes what is given in Fig. 74, and this has been justified by the results obtained from about sixty experiments at a saw-mill.

17. On the Surface Temperature.

If the surounding medium be the same as the drying substance, the equation (31) may be satisfied completely. But actually the substance is surrounded by the atomosphere of lower temperature, and the surface temperature of it is lower than that of its center, because, in the case of such substance as wood or clay, heat must go through a bad conductor of heat before it can reach the surface. If an element of volume along the surface of the substance be assumed, and its temperature increase by $d\theta$ degrees Centigrade in the lapse of a given time dt, the

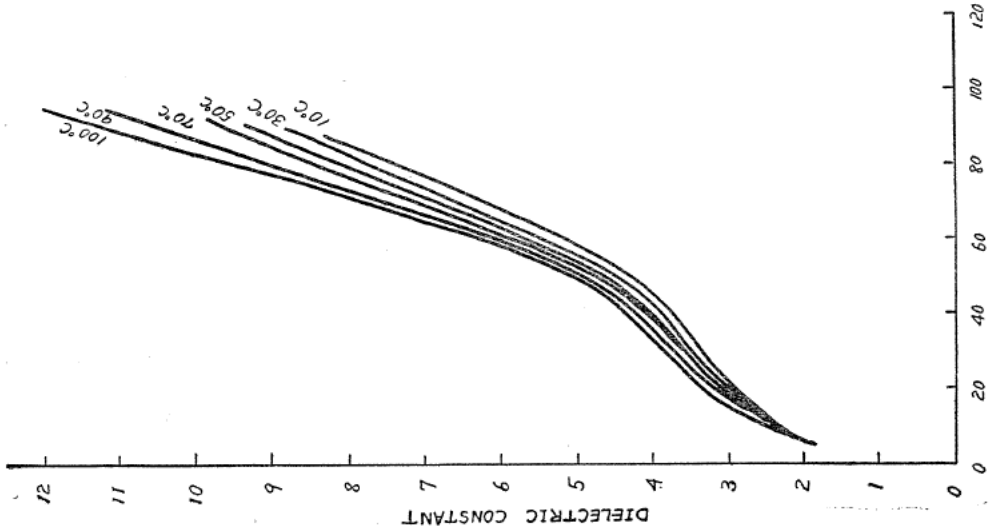

FIG. 69. Japanese Cedar. (Frequency, 5 MC.)

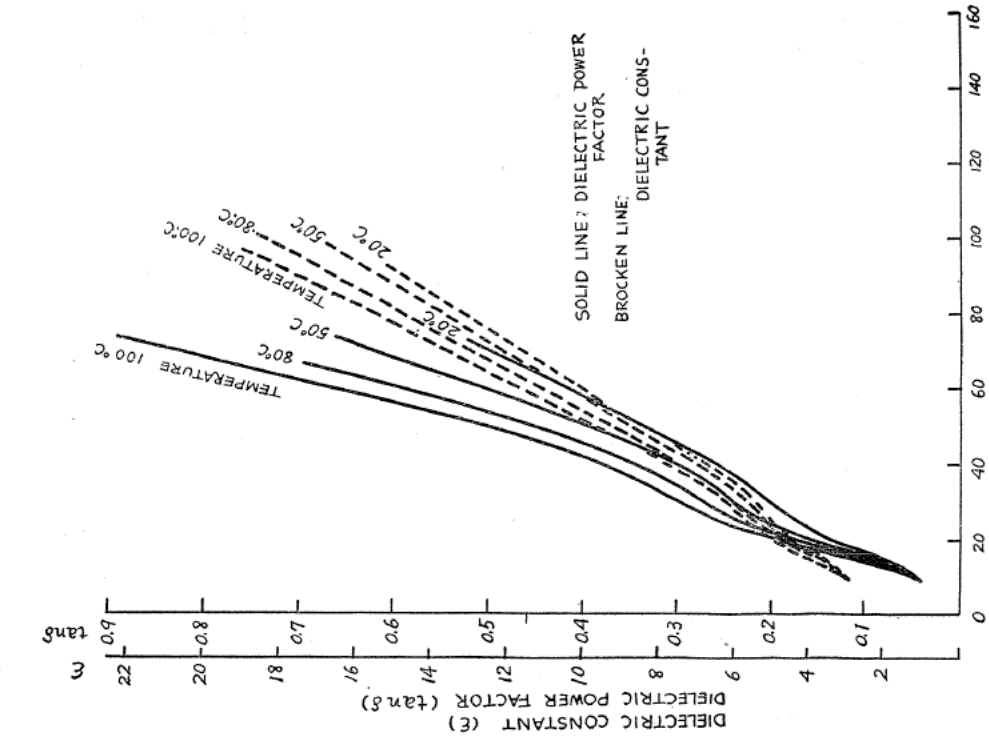

FIG. 71. Japanese Cypress. (Frequency, 5 MC.)

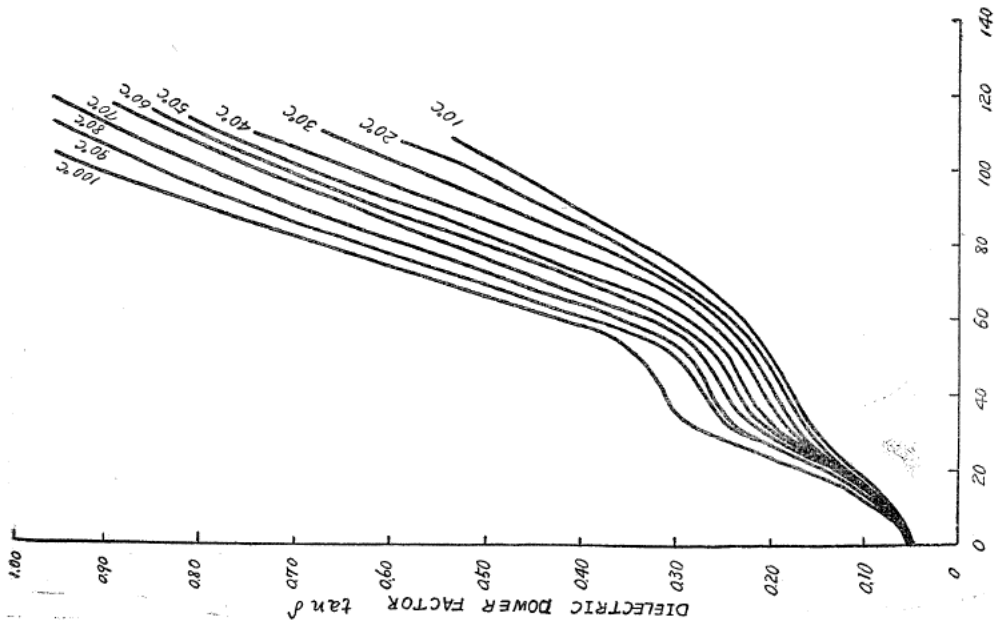

. 70. Japanese Cedar. (Frequency, 5 MC.)

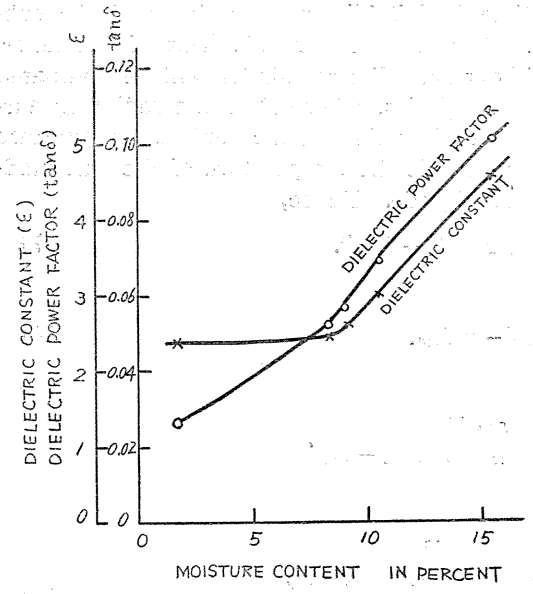

← FIG. 72. *Cercidiphylum Japonicum.* (Frequency, 5 MC.)

↓ FIG. 73. *Quercus glandulifera* (oak). (Frequency, 5 MC.)

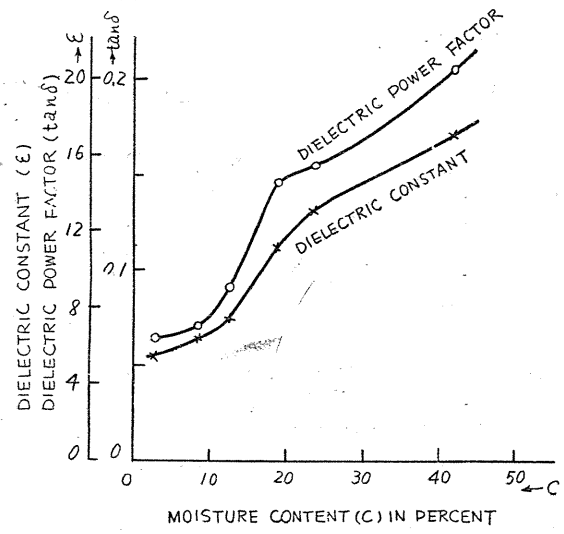

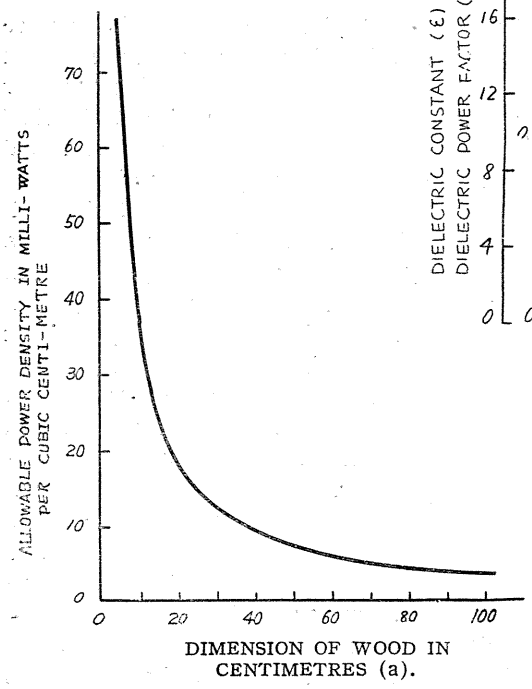

← FIG. 74

amount of heat liberated during this time is Qdt kilogram-calories, and the substance absorbs $s\rho d\theta$ kilogram-calories, where s is the specific heat of substance, and ρ the weight of the substance in kilogram. The remainder will be dissipated to the amount of $A\alpha(\theta_s-\theta_0)dt$ kilogram-calories, where A is the radiating surface in square centimeter, α the coefficient of cooling, θ_s the surface temperature of the substance in degrees Centigrade and θ_0 is the temperature of the surrounding medium or atmosphere in degrees Centigrade. Hence,

$$Qdt = s\rho d\theta + A\alpha(\theta_s-\theta_0)dt. \tag{37}$$

From the equation (27)

$$Q = H - w_l H_w. \tag{38}$$

Therefore,

$$dt = \frac{s\rho \cdot d\theta}{(H - w_l \cdot H_w) - A\alpha(\theta_s-\theta_0)}.$$

Assuming that $\theta_s = \theta_0$ when $t = 0$,

$$\begin{aligned} \int_0^t dt &= s\rho \int_{\theta_0}^{\theta_s} \frac{d\theta}{(H - w_l \cdot H_w) - A\alpha(\theta_s-\theta_0)} \\ \theta_s - \theta_0 &= \frac{(H - w_l \cdot H_w)}{\alpha A} \cdot \left(1 - \varepsilon^{\frac{\alpha A}{s\rho} t}\right). \end{aligned} \tag{39}$$

And when $t = \infty$,

$$(\theta_s - \theta_0)_{t=\infty} = \frac{H - w_l \cdot H_w}{\alpha A}. \tag{40}$$

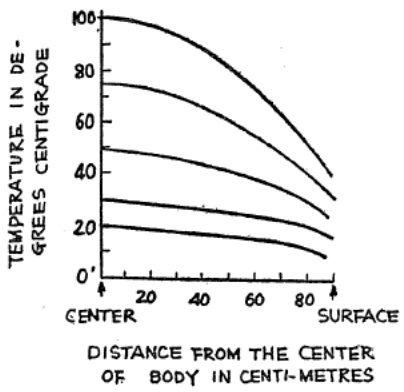

FIG. 75

But when a test piece was dried, the surface temperature differed from what the equation (40) shows, owing to the evaporation of water from it. In our experiment with a cylindrical test piece of clay (its diameter 68 cm. and 20 cm. in height), the temperature distribution during the drying period was found to be such as is shown in Fig. 31, which shows that the surface temperature is considerably lower than that at the center. This result is only that of the experiment with a small test piece, but also from our experiment made with plywood of greater volume (184 cm × 95 cm × 85 cm.), we have obtained a similar result (Fig. 75). In any case we find that the surface temperature is considerably lower than that at the center. When the *Cercidiphylum Japonicum* wood with the volume of 3.5 cubic meters was dried with the radio-frequency power of about 14 kilowatts (oscillater input being 27 kilowatts and the frequency 5 MC), the surface temperature rose to about 70 degrees Centigrade. (It was measured with an alcohol thermometer, which can show only the approximate value.) When the electric power or the room temperature was slightly increased, the "internal explosion" took place. Hence, the maximum

internal temperature in this case must be much higher than that at the surface as before described. From this experiment, it is seen that the phenomenon of "internal explosion" will be caused by the maximum internal pressure which depends on the sum of the maximum internal temperature rise and the room temperature, or, the maximum temperature itself. Therefore, we must take into consideration the room temperature as well as the internal temperature rise in radio-frequency heating.

18. On the Surrounding Condition or the Fundamental Idea in Desighing a Drying Room.

When drying, we must be attentive to the surrounding condition, especially the temperature, the humidity and the atmospheric current. Temperature has been dealt with above, and the other two factors remain to be considered.

It is difficult to discuss the effect of the atomospheric current, but it has been experimented by other authorities. For instance, when the water evaporates gently from the surface of a body, the rate of evaporation (w_s) is indicated as follows:[7]

$$w_s = 0.927(C_0 - C)\sqrt{\eta \cdot x \cdot U}, \tag{41}$$

where δ: thickness of the vapor skin on the surface of body,
C_0: vapor concentration at $\delta = 0$,
C: vapor concentration at $\delta = \delta$ cm.,
η: coefficient of viscocity of vapor,
U: velocity of the atmospheric current,
x: length along the surface of body.
(Figures are all in C.G.S. units.)

As vapor concentration is proportional to the vapor pressure, we can put

$$w_s = B(p_s - p_0), \tag{42}$$

where, p_s: vapor pressure at the surface of body,
p_0: vapor pressure at the surrounding medium,
B: a constant.

If the rate of surface evaporation is larger than that of internal diffusion of water within the substance to be dried, and when the thermal stress exceeds the mechanical strength of the substance, the surface cracks may appear. To avoid this surface crack, the rate of surface evaporation must be balanced with that of internal diffusion, that is,

$$w_s = w_l, \tag{43}$$

$$B(p_s - p_0) = \frac{n\pi r^4}{8\eta l}(p_{\max} - p_s), \tag{44}$$

$$p_0 = p_s - \frac{n\pi r^4}{8\eta l B}(p_{\max} - p_s). \tag{45}$$

In this case, the mechanical strength of the substance does not considered. Hence, we know that the drying-room pressure may be lower than p_0, that is, it may be practically as low as the saturated vapor pressure of about 50 degrees Centi-

grade as described following. For example, when four cubic meters of oak is loaded in the drying room of concrete (6 meter × 2.7 meter × 3.3 meter) and the electric power of 35 kilowatts (oscillator input and frequency 5.5 MC) is applied, the termperature of the surface of wood becomes to 65 degree Centigrade and the room temperature to 63 degree Centigrade and drying room pressure also to the saturated one of 63 degree Centigrade. In this state, the wood does not dried satisfactory and the vapor in the room must be escaped out and it is proper to make the difference in vapor pressure between the surface of wood and the room about 0.2 kilo-gram per square centimeter, i.e. the suitable value of room pressure is the saturated one of about 50 degree Centigrade. Also, it is ascertained from the experimental results in practice that about 70 degree Centigrade is suitable for the surface temperature of wood and the saturated pressure of (45 ~50) degree Centigrade for the room pressure. This condition can be easily brought by water evaporating from the wood itself in the radio-frequency drying and other heat source, such as a steam boiler or electric heater, scarcely needs. If the surrounding temperature is increased by other heat source, the maximum internal pressure (p_{max}) in wood increases as before described and "internal explosion" will take place. Hence, the room temperature should be lower in the radio-frequency drying. (When the electric power is lower too small, the "internal explosion" can be avoided, but drying velocity lower and the electric potential falls exceedingly at the surface of wood and the temperature of the surface increases and "case hardning" may take place as described in page 22.)

19. On the Drying Period.

The accurate calculation of the drying period is difficult, but an approximate value can be calculated as follows. As stated above (see Fig. 3), the drying period consists of the pre-heating, the constant drying rate and the decreasing drying rate periods. From the heating and cooling characteristics of the substance, it can be seen that the drying rate during the pre-heating period can be expressed by the equation,

$$w_l(1-\varepsilon^{-t/T_0}),$$

where, T_0 is the time constant.
And that the rate during the drying period is constant and equal to w_l, and for the decreasing drying rate period this rate can be expressed by the equation,

$$w_l \cdot \varepsilon^{-t/T_0}.$$

When a piece of wood is to be dried from the moisture content of $c\%$ to $c_0\%$, we must take away so much water as makes the difference between those states. According to J. A. Newlin and T. R. C. Wilson,[8] the relation between wet volume and dry volume is

$$V_0 = V(1-0.28\,g), \tag{46}$$

where, V_0: volume of wood at the moisture content 0%,
V : volume of wood at the fiber saturation point,
g : specific gravity of wood.
Hence, the water contained in wood of the moisture content $c\%$ is

$$V_0 \cdot g \cdot \frac{c}{100} = V(1-0.28) \cdot g \cdot \frac{c}{100} \text{ grams.} \tag{47}$$

As the volume of wood shrinks from the fiber saturation point (c_c%), or the critical moisture content, the amount of water to be taken away until the fiber saturation point is reached, is

$$(1-0.28\,g) \cdot gV \cdot (c-c_c)/100 \text{ grams,} \tag{48}$$

and when wood is to be dried from the fiber saturation point till c_0% is reached, then the amount of water to be taken away, is

$$(1-0.28\,g) gV \cdot (c_c - c_0)/100 \text{ grams.} \tag{49}$$

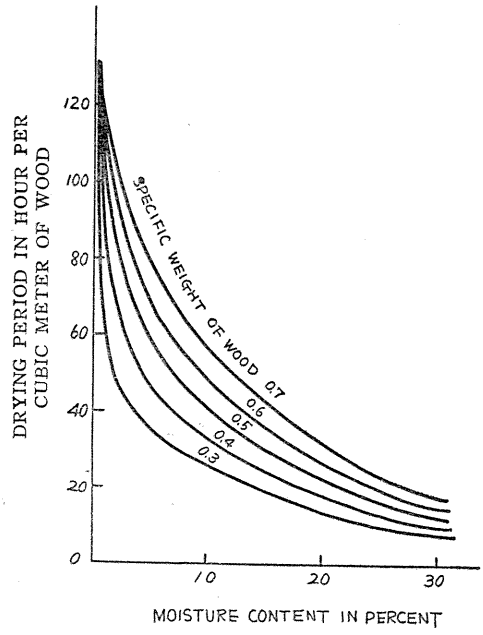

FIG. 76

If we assume the drying rate to be equal to the flowing rate of the water (w_l) coming out from the capillary system which is described above (see equation (14)), the drying period can be calculated as follows: If the drying rate at the pre-heating period increases linearly, the drying period until the critical moisture content is nearly equal to

$$\frac{(1-0.28\,g)(c-c_c)Vg}{100\,w_l} + \frac{T_0}{2}, \tag{50}$$

and the drying period from the critical moisture content to c_0% is t_α seconds, which is calculated as follows.

$$\frac{(1-0.28\,g)gV(c_c-c_0)}{100} = \int_0^{t_\alpha} w_l \cdot \varepsilon^{-\frac{t}{T_0}}\,dt, \tag{51}$$

$$t_\alpha = -T_0 \log\left\{1 - \frac{(1-0.28\,g)gV(c_c-c_0)}{100\,w_l T_0}\right\}. \tag{52}$$

Hence, the drying period from the moisture content of c% to c_0% is

$$t_{\text{total}} = \frac{(1-0.28\,g)gV(c-c_c)}{100\,w_l} + \frac{T_0}{2} - T_0 \log\left\{1 - \frac{(1-0.28\,g)gV(c_c-c_0)}{100\,w_l T_0}\right\}. \tag{53}$$

If we calculate by this equation the drying period of wood, the result shown in Fig. 76 is obtained.

20. On the Practical Data Concerning Radio-Frequency Heating.

1) *Drying of Wood.*

The practical data concerning wood-drying are given in Fig. 77 and the distribution of the moisture content during the drying period is shown in Fig. 51. The electrical characteristic measured in the circumstance under which these data were gathered is shown in Fig. 78, and Fig. 79 shows the frequency variations

during the drying period.

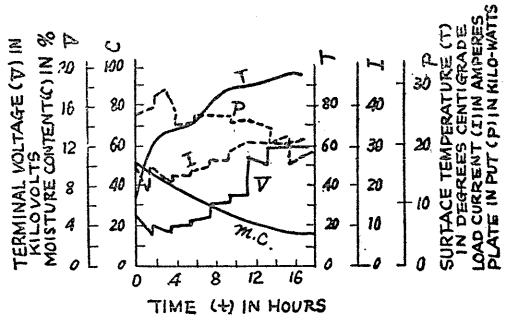

FIG. 77

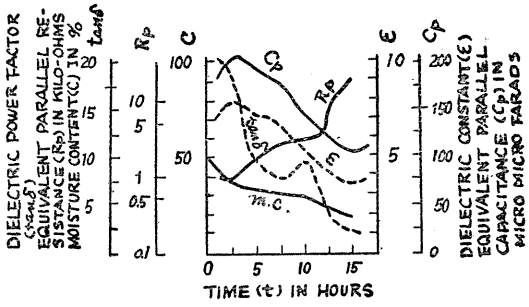

FIG. 78

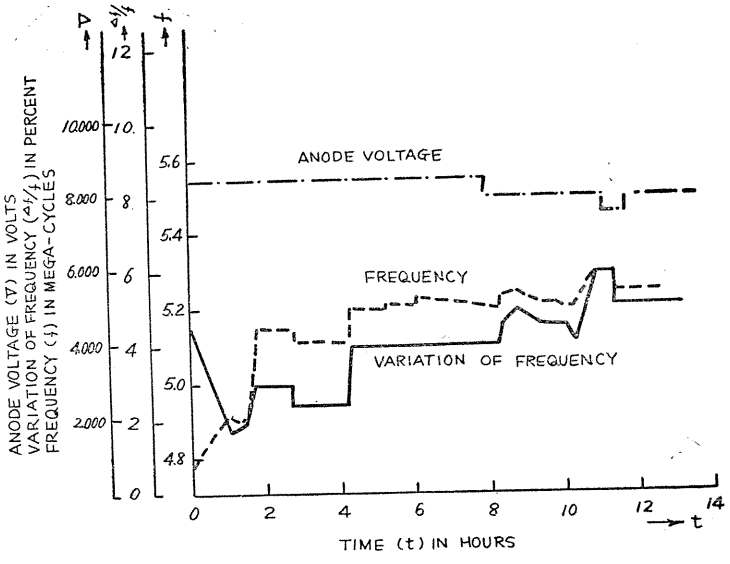

FIG. 79

2) *Drying of Textiles.*

When a cylinder of textiles was dried by radio-frequency heating, the results

shown in Fig. 80 and Fig. 81 were obtained. When the drying characteristics of other textiles such as melton and serge were examined, the results shown in Figs. 82 and 83 were obtained respectively. Next, when we measured the dielectric characteristics of such material as wood, viscose, rayon, melton and serge with the Q-meter or by the differential condenser method, we obtained the results shown in Figs. from 84 to 86 respectively.

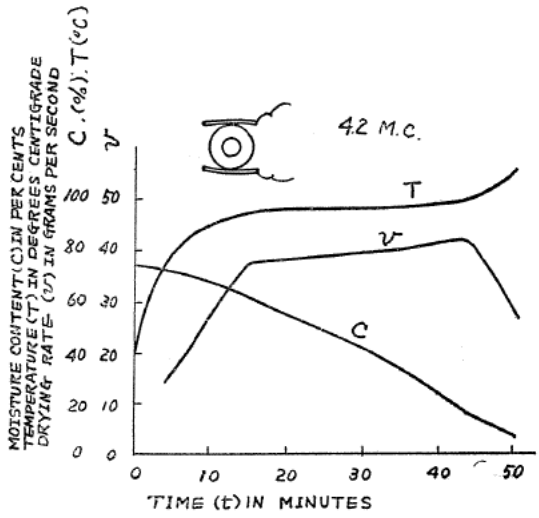

FIG. 80

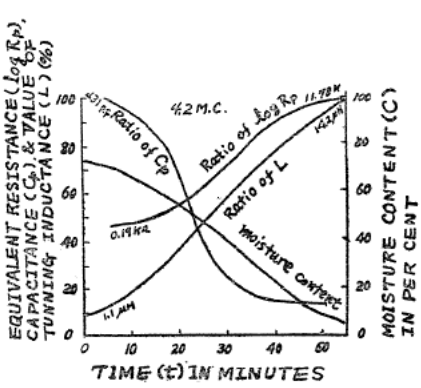

FIG. 81

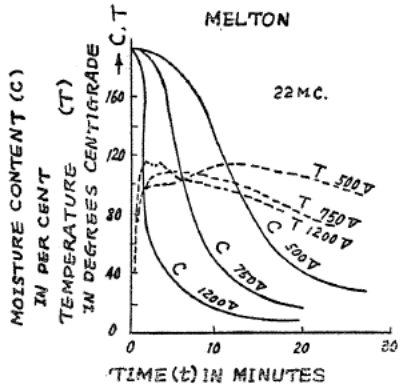

FIG. 82

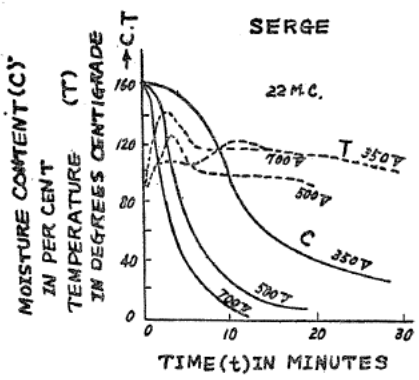

FIG. 83

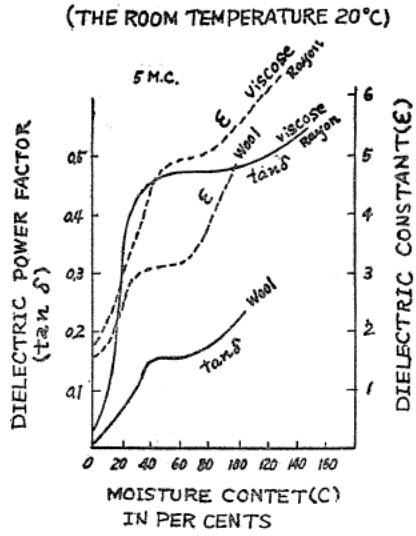

FIG. 84

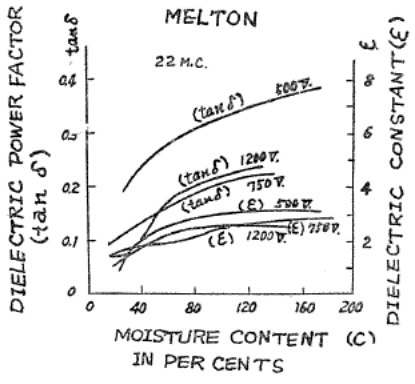

FIG. 85

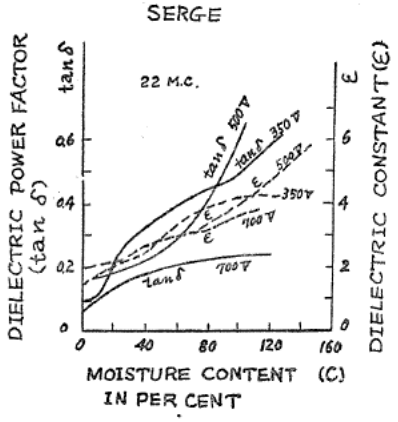

FIG. 86

21. Conclusions.

1) Radio-frequency heating is more favorable for drying bad conductors of heat than oven-heating.

2) In radio-frequency drying, what we must be watchful against above all is the phenomenon of "internal explosion." The "surface crack" in this case is not so serious a thing as in oven-drying and it can be avoided by modifying surface evaporation as before described.

3) The internal pressure distribution of the drying substance is complicated, and the maximum internal pressure appears at the decreasing drying rate period, or at the end of the constant drying rate period. What features the internal pressure will present depends on the physical properties of the drying substance.

4) Clay which has generally been considered as uniform substance, is not uniform but it is a capillary system. Hence, the discussion of the drying mechanism of some substance as clay should be based on the supposition that it is a capillary system instead of uniform material.

5) The allowable internal pressure must be lower than the mechanical strength of the substance to be dried, and the allowable electric power density and the capacity of the radio-frequency drying apparatus can be calculated from it.

6) It is important in radio-frequency drying that the surrounding room temperature should be considerably lower than that of the substance dried, and the vapor pressure of the surrounding atomosphere should be kept at the saturated pressure of the room temperature.

Acknowledgment.

Grateful acknowledgment must be made here to Mr. Shigekatsu Otori and Mr. Koji Iwata, who made this research conjointly with me, for their most earnest and sincere assistance in these experiments, and also to the students—Mr. Tooru Okada, Mr. Shūhei Shibata and Mr. Kōji Suzuki—for the assistance they willingly offered, and this research was performed with the fund of scientific research of the educational department of Japan.

Ukichi Shinohara.

References.

1) S. Kamei, S. Kato and Y. Takeya: Latest Radio-Frequency Application. (I) (comdlied by Yamamoto) 102, (1949).
2) E. S. Winlund: Electronics. 108, (1946).
3) G. H. Brown, C. N. Hoyler and R. A. Bierwirth: Theory and Application of Radio-Frequency Heating. 13, (1949).
4) J. Duclaux and J. Errera: Rev. Gen. Colloides. 3, 97 (1925).
5) Mechanical Handbook of I.M.E. of Japan. 1063, (1939).
6) L. E. Wise: Wood Chemistry. 76, (1946).
7) I. Oshida: Evaporation and Drying, (Kawade Ltd.) 53, (1950).
8) J. A. Newlin and T. R. C. Wilson: U. S. D. Agr. Bull. 676, (1919).